The nuclear optical model

The nuclear optical model

P E HODGSON

Nuclear Physics Laboratory, University of Oxford, Oxford

Contents

Abstract. The main features of the nuclear optical model are reviewed, with particular attention to current growth points. The determination of the form and strength of the nucleon–nucleus interaction by calculation from the nucleon–nucleon interaction is described and the results compared with those obtained phenomenologically. The potential is applied to analyse single-particle bound states, and it is shown how this can give its isospin and state dependence. Even when it is used simply to calculate the elastic scattering, the optical model must be established in the framework of nuclear reaction theory, and allowance made for the effects of all the reaction channels, and in particular for the compound nucleus processes and the associated fluctuations in the cross sections. The model can then be applied to analyse data on the elastic scattering of nucleons, deuterons, helions, tritons and α particles by nuclei, and this enables its parameters to be determined more precisely and its range of validity to be investigated. The nucleon data is so extensive that it is possible to study several small terms in the potential, in particular the isospin term and the nuclear spin term, in addition to the familiar spin–orbit term. The scattering of the composite particles shows several apparently anomalous features that on investigation yield additional information on nuclear structure. The optical model may be extended to give the inelastic as well as the elastic scattering, and this makes it possible to analyse many apparently complicated phenomena. The application of the results of optical model analyses to the calculation of compound nucleus cross sections is also discussed, together with the use of optical model wavefunctions in calculations of direct reaction cross sections.

This review was completed in August 1971.

1. Historical introduction and summary

It is about twenty years since it was first suggested that the interaction of nucleons with nuclei could be represented by a complex potential, and since then it has been developed into a model of considerable power and generality. A wide range of scattering data can be accounted for by the model to a high degree of

precision, and the corresponding wavefunctions are extensively used to extract information on nuclear structure from measurements of nuclear interaction cross sections.

In this review, the historical development of the optical model is briefly summarized, and the special features of its application to a variety of scattering problems are described. The main emphasis is on the physical ideas rather than on the mathematical techniques necessary for realistic calculations, but references to specialized treatments are given whenever appropriate.

The essential idea of the optical model is that a nucleon incident on a nucleus may be elastically scattered or it may cause a variety of different reactions. If the incident particle is represented by a wave, then in classical language it may be scattered or it may be absorbed. In optics this is analogous to the refraction and absorption of a light wave by a medium of complex refractive index, and just as the imaginary part of the refractive index takes account of the absorption of the light wave so in the nuclear case the imaginary part of the complex potential describing the interaction takes account of all the nonelastic reactions.

This simple idea was applied in a semiclassical way by Fernbach *et al* (1949) to the interpretation of the data on the scattering and absorption of 90 MeV neutrons by a range of nuclei. It was found that the total elastic and the total reaction cross sections could be well accounted for, and the real and imaginary parts of the potential were in qualitative accord with crude semiclassical estimates based on the nucleon–nucleon cross sections. A full quantum mechanical calculation of the scattering of 17 MeV protons by aluminium using a complex potential to represent the proton–nucleus interaction was made by Le Levier and Saxon (1952), and gave a good account of the rather imprecise data available at that time.

It is an essential feature of the model that nuclei are regarded as blobs of nuclear matter whose properties are determined by their size (or equivalently by the number of nucleons comprising them, since nuclear matter is almost incompressible), apart from certain small structure effects that will be mentioned in more detail later. This implies that the same potential can account for the interaction of particles of different energies with different nuclei. To the extent that this can be done, the optical model is at least a useful way of summarizing a vast body of experimental data.

If this is to be so, then the experimental data should show a regular variation with energy and atomic number, and at first sight this seems very unlikely because nuclei have very different structures, as shown by their energy level diagrams. Indeed, if measurements are made at high resolution the cross sections often show an extremely complicated and characteristic structure. If, however, the energy-averaged cross sections are examined, and these may be obtained at once from low-resolution measurements, a systematic behaviour becomes apparent. This was first shown by the neutron cross sections of Barschall (1952) (see figure 1). The energy-averaging of cross sections is thus an essential feature of the model at low energies when compound nucleus reactions are appreciable.

It was then found by Feshbach *et al* (1954) that the overall variation of these neutron cross sections with atomic weight could be represented very well by a complex neutron–nucleus potential of the form

$$\begin{aligned} V &= V_0(1+i\zeta) \qquad \text{for } r<R \\ &= 0 \qquad\qquad\quad \text{for } r>R \end{aligned} \tag{1.1}$$

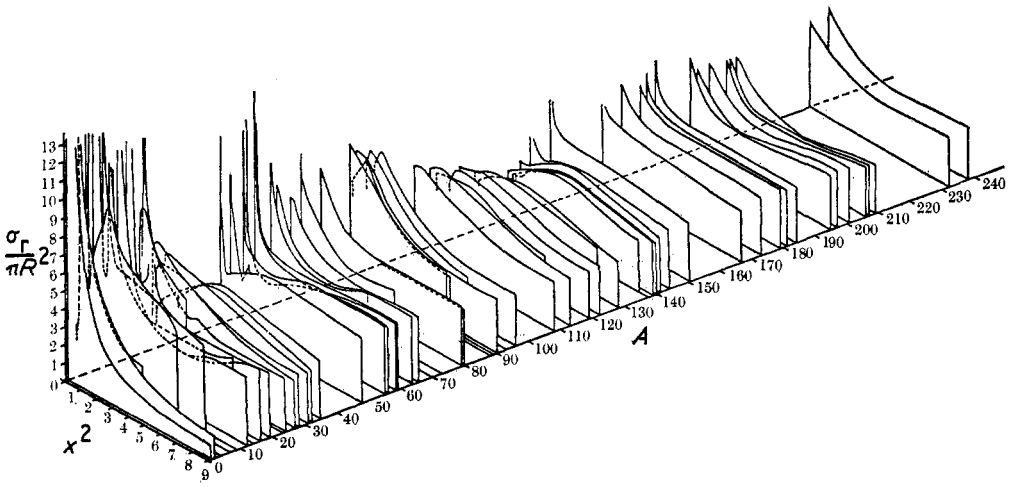

Figure 1. Observed neutron total cross sections as a function of energy and mass number, radius $R = 1{\cdot}45A^{1/3}$. From Feshbach *et al* (1954).

where $R = 1{\cdot}45 \times A^{1/3}$ fm, $V_0 = 42$ MeV, $\zeta = 0{\cdot}03$ and A is the atomic mass. The results of their calculations are shown in figure 2.

This spectacular success established the usefulness of the optical model, and thereafter it was soon applied to a wide range of nuclear interactions. As the precision of the data increased the model was refined so that it can now account not only for differential and reaction cross sections but also for polarizations to a high degree of accuracy. Many measurements have also been made of the elastic scattering of composite particles by nuclei and, as the cross sections show the same

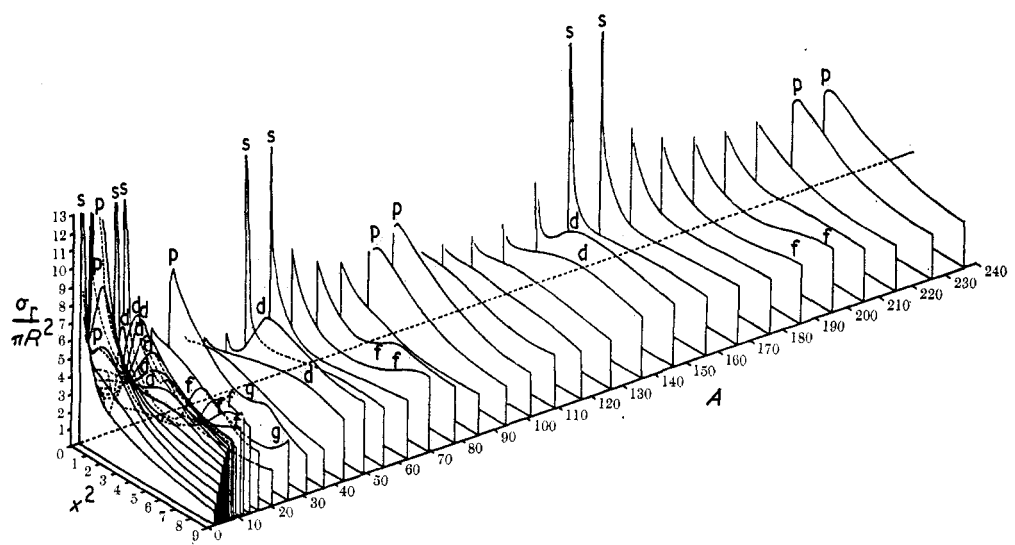

Figure 2. Calculated neutron total cross sections as a function of energy and mass number, for a potential depth $V_0 = 42$ MeV, radius $R = 1{\cdot}45A^{1/3}$, $\zeta = 0{\cdot}03$. The energy ϵ is expressed in terms of $x^2 = A^{2/3}\,A/10(A+1)\,\epsilon$, where ϵ is in MeV. From Feshbach *et al* (1954).

overall features and regularities as the corresponding nucleon cross sections, the optical model was applied to them as well, with similar success.

Apart from the rather crude basis provided by the semiclassical optical model all this work is essentially phenomenological, in that the values of the parameters of the optical potentials are found by optimizing the fit to the experimental data. But while the model can be used in this way it is desirable to put it on a more fundamental basis, and to derive it as far as possible from the known properties of the nucleus and of the nucleon–nucleon interaction. This is desirable not only to unify our theory of nuclear reactions but also to resolve certain difficulties and ambiguities in purely phenomenological analyses of data of high precision. The problem of calculating the optical potential is evidently an exceedingly complex one, since all the interactions of the incident particle with the nucleons of the target must be included. Brueckner's (1954) theory of nuclear matter was an important step forward, and Feshbach's formalism provided a useful framework for a theoretical definition of the potential. Their work established certain important features of the optical potential, in particular its nonlocality, but was unable to define its form and strength with sufficient precision. A simpler approach by Greenlees *et al* (1969) using realistic forms for the nuclear matter distribution and the nucleon–nucleon interaction gave good quantitative results, and subsequent work by Kidwai and Rook (1971) has justified the assumptions of Greenlees *et al* (1969) by a nuclear matter calculation similar to that of Brueckner. This work is summarized in § 2.

The optical model can be considered as an extension to positive energies of the nuclear shell model, so that there is a physical continuity between the shell model potential for nucleons of negative energies and the real part of the optical potential at positive energies. The single-particle states of nuclei can be used to determine the shell model potential, and this brings out certain features that are not readily obtainable from the analysis of scattering data. This work is described in § 3.

In order to use the optical model to analyse experimental data it is necessary to see how the elastic scattering cross sections obtained from the model are related to all the other reactions that may occur. In particular the role of energy-averaging needs to be precisely expressed in relation to the experimental conditions and the components of the cross sections. This is considered in § 4.

With the theoretical understanding provided by the optical model formalism, it is possible to make detailed analyses of experimental data and thus to confirm its usefulness and determine its parameters to a high degree of precision. The mathematical and computational techniques necessary to do this are summarized in § 5.

A vast body of experimental data for the elastic scattering of neutrons and protons by nuclei is now available, and many phenomenological optical model analyses have been made of the differential cross sections and polarizations, together with the associated reaction and total cross sections. The analyses give information on the energy dependence of the optical potential and on the way it depends on nuclear structure. These analyses are summarized in § 6.

The application of the optical model to the elastic scattering of composite particles, in particular deuterons, helions, tritons and α particles, presents many features that are of interest both for nuclear reactions and for nuclear structure. The corresponding optical potentials are not as well defined as for nucleons, but nevertheless some success has been achieved in calculating them from the constituent nucleon–nucleus interactions. Their stronger absorption and higher

mass-to-charge ratios relative to those of protons give rise to special features that are discussed for deuterons in § 7, for helions and tritons in § 8 and for α particles in § 9.

The formal theory of nuclear reactions shows that the wavefunctions in all the open reaction channels satisfy a set of coupled differential equations, one for each channel. This set is too large to solve in practice, so it is severely truncated, and the effect of the channels not considered is taken into account by allowing the interaction potential to become complex. The most extreme truncation, that which retains only the equation for the wavefunction in the shape elastic channel, gives the usual optical model. A less severe truncation retains one or more equations for wavefunctions in nonelastic channels, and this enables both the elastic and nonelastic cross sections to be calculated simultaneously, provided a model is available for the channels considered, and for the corresponding interaction potentials. This approach is a significant improvement over the perturbation theory calculation when the coupling between the elastic and the nonelastic channels chosen is strong, and as this is most often the case for inelastic scattering with the excitation of collective states, these have most frequently been treated by the coupled-channels method. Since this is a natural extension of the optical model it is briefly considered in § 10.

The energy-averaged elastic scattering cross sections all contain a compound nucleus component, which may be important or negligible depending on the conditions. The optical model enables this to be calculated by the methods described in § 11.

Optical model wavefunctions are widely used in reaction calculations, and some of the attendant uncertainties and possible ways of overcoming them are considered in § 12.

Finally in § 13 the present state of optical model calculations is reviewed, and some lines of future development are indicated.

The nuclear optical model and its relation to other theories of nuclear reactions is discussed in more detail by Hodgson (1971). The present review concentrates on the essential physical ideas of the model with attention to some current growth points and unresolved problems.

Throughout this review, all distances are in fermis (1 fm = 10^{-13} cm) and energies in MeV.

2. The nucleon-nucleus interaction

In their pioneer work on the optical model, Feshbach *et al* (1954) used the square-well potential (equation (1.1)). This is clearly unphysical, and indeed calculations soon showed that the high reflectivity of such potentials gives absorption cross sections that are far too small. A rounded potential is clearly preferable, and since the nucleon–nucleon potential falls off exponentially at large distances it is reasonable to expect the optical potential that results from a sum of such interactions to do the same. It is also desirable to retain the feature of the square-well potential of constancy in the nuclear interior since this is to be expected from the short-range and saturation character of nuclear forces which ensures that once a nucleon is within the nucleus it experiences on the average no resultant force.

These features are conveniently represented by the Saxon–Woods form factor

$$f(r) = \frac{1}{1+\exp\{(r-R)/a\}} \tag{2.1}$$

where R is the radius parameter and a the surface diffuseness parameter. Since the nuclear radii are approximately proportional to $A^{1/3}$ it is usual to take out most of this dependence by putting $R = r_0 A^{1/3}$, while recognizing that the parameter r_0 may still have a weak dependence on A. These arguments only apply to the real part of the potential, but for convenience the same radial dependence was used in earlier calculations for the imaginary part as well. Subsequent work, outlined in § 6, has indicated substantial differences between the form factors of the real and imaginary parts of the potential.

The observation that elastically scattered nucleons are usually polarized implies that the optical potential is spin dependent, and, of the variety of possibilities, the spin–orbit form, familiar from the shell model, is the most convenient. Analogy with the spin–orbit force in atoms, substantiated by nuclear matter calculations, indicates the explicit form, applicable to particles of spin $\frac{1}{2}$

$$V_{\mathrm{S}}(r) \equiv V_{\mathrm{S}}\, f_{\mathrm{S}}(r) = V_{\mathrm{S}}\left(\frac{\hbar}{m_\pi c}\right)^2 \frac{1}{r}\frac{\mathrm{d}f(r)}{\mathrm{d}r} \boldsymbol{L}.\boldsymbol{\sigma} \tag{2.2}$$

and this is able to account for most of the polarization data. More complicated forms of spin dependence are used for particles of spin greater than $\frac{1}{2}$ (see § 7). These simple considerations are adequate to establish the phenomenological form of the potential, and the parameters may be determined by systematically optimizing the fit to the experimental data, using the methods of § 5.

In practice it is frequently found that many sets of parameters give equally good fits to the data, and the question then arises whether any one of these is more physical than the others and if so which is to be preferred.

These parameter ambiguities, as they are called, are of two main types, discrete and continuous. Discrete ambiguities refer to regions of parameter space that give acceptable fits separated by unacceptable regions. The most notable example of this is the potential depth ambiguity, in which it is found, particularly for composite particles, that a whole series of potentials of increasing depth (eg 50, 100, 150 ... MeV,) give almost equally good fits, the other parameters remaining the same. Continuous ambiguities refer to combinations of parameters that may be simultaneously varied subject to some constraint without significantly affecting the fit. The most notable examples of this type are the Ur_{u}^2 and Wa_{w} ambiguities in nucleon scattering; provided these products are kept constant, the individual parameters may be varied by as much as 20–30% without affecting the fit. The existence of these and other more complicated parameter ambiguities means that it is not possible to establish the optical potential by phenomenological analyses alone. It is necessary to start by constraining the potential as closely as possible by physical requirements *before* parameter optimization. This is not easy, as the physical constraints depend on complex many-body calculations, and even then there is no guarantee that they will be just adequate to resolve the ambiguities without adversely affecting the fits.

Discrete ambiguities do not occur for nucleons, since the depth of about 50 MeV appropriate to the shell model must be the physical one. In the case of deuterons and, to a lesser extent, helions, tritons and α particles the discrete ambiguities may be resolved by calculating the potential from the constituent nucleon–nucleus interactions. This is discussed more fully in the appropriate sections. Continuous ambiguities are more difficult to resolve, and it is usual to sidestep most of the trouble they cause by using standard values for the form factor

parameters. This at least makes it possible to compare the potentials obtained from different analyses. Further progress thus requires a detailed theory of the optical potential in terms of the constituent nucleon–nucleus interactions. This is clearly a very difficult many-body problem, but substantial progress has been made by Brueckner (1954) and his colleagues and by Bethe (1956). The formal theory of nuclear reactions developed by Feshbach (1958, 1962) enables the contributions to the optical potential to be identified, but it is not very amenable to practical evaluation.

It would require a separate review to consider these theories in detail, but it is useful to indicate very briefly the essentials of Feshbach's formalism, as this clarifies several key features of the optical potentials. It enables the optical potential to be expressed in terms of the unperturbed hamiltonian H_0 and the potential $V(\boldsymbol{r}_0, \boldsymbol{\xi})$ between the incident particle and the target nucleus, where $\boldsymbol{r}_0$ is the position of the incident particle and $\boldsymbol{r}_1, \ldots, \boldsymbol{r}_A\ (\equiv \boldsymbol{\xi})$ those of the particles in the target nucleus. The optical potential describes only the elastic scattering, but since the nonelastic processes remove flux from the elastic channel they must be taken into account as well. In addition there are higher-order processes, such as the excitation of virtual states and their subsequent de-excitation back to the elastic channel, that also contribute to the elastic scattering amplitude, so that the excited states $\phi_n(\boldsymbol{\xi})$ of the target must also be taken into account. The other channels involving transfer reactions can also contribute, but they are omitted here for simplicity, so that we consider only inelastic scattering.

The total hamiltonian is given by

$$H = H_0 + V(\boldsymbol{r}_0, \boldsymbol{\xi}) = H_0(\boldsymbol{\xi}) + T(\boldsymbol{r}_0) + V(\boldsymbol{r}_0, \boldsymbol{\xi}) \tag{2.3}$$

where $H_0(\boldsymbol{\xi})$ is the target hamiltonian and $T(\boldsymbol{r}_0)$ the kinetic energy of the incident particle. The total wavefunction Ψ satisfies the equation

$$(H - E)\,\Psi = 0 \tag{2.4}$$

and the unperturbed wavefunction Φ satisfies the equation

$$(H_0 - E)\,\Phi = 0. \tag{2.5}$$

Neglecting the requirements of antisymmetrization, Ψ may be expanded as a series of products of the wavefunction $\psi_\alpha(r_0)$ of the incident particle and the corresponding states of the target nucleus

$$\Psi(\boldsymbol{r}_0, \boldsymbol{\xi}) = \sum_\alpha \psi_\alpha(r_0)\,\phi_\alpha(\xi) \tag{2.6}$$

when the $\psi_\alpha(r_0)$ satisfy the equation

$$(T + \mathscr{V}(r_0) - \epsilon_\alpha)\,\psi_\alpha(r_0) = 0 \tag{2.7}$$

where $\mathscr{V}(r_0)$ is the optical potential and $\epsilon_\alpha = E - E_\alpha$, E_α being the excitation energy of the target nucleus.

We now define the operator P that projects from the total wavefunction only the ground state part of the target wavefunction

$$P\Psi = \Phi_0 = \phi_0\,\psi_0(r_0) \tag{2.8}$$

and also the operator

$$Q = 1 - P. \tag{2.9}$$

These operators satisfy the relations

$$P^2 = P, \quad Q^2 = Q, \quad PQ = 0. \tag{2.10}$$

Insertion of the unit operator in (2.4) gives

$$(H-E)(P+Q)\Psi = 0. \tag{2.11}$$

Multiplying by P and Q in turn and using (2.10) gives coupled equations for $P\Psi$ and $Q\Psi$

$$(E-PHP)P\Psi = PHQQ\Psi \tag{2.12}$$

$$(E-QHQ)Q\Psi = QHPP\Psi. \tag{2.13}$$

The latter equation may be solved formally to give

$$Q\Psi = \frac{1}{E-QHQ+i\epsilon}QHPP\Psi \tag{2.14}$$

where the term $+i\epsilon$ is a reminder that only outgoing solutions are required. In the subsequent formalism it will be omitted for convenience. Substitution of (2.14) in (2.12) gives a formal equation for the wavefunction in the incident channel,

$$\left(E-PHP-PHQ\frac{1}{E-QHQ}QHP\right)P\Psi = 0. \tag{2.15}$$

Taking the ground state of the target nucleus as the zero of energy

$$H(\xi)\phi_0 = 0 \tag{2.16}$$

and using the explicit expression for P

$$P = |\phi_0)(\phi_0| \tag{2.17}$$

where the curved brackets indicate dependence on the ξ coordinates only, gives

$$\begin{aligned} PHP &= |\phi_0)(\phi_0|H(\xi)+T+V|\phi_0)(\phi_0| \\ &= |\phi_0)\{T+(\phi_0|V|\phi_0)\}(\phi_0| \end{aligned} \tag{2.18}$$

and

$$\begin{aligned} PHQ &= |\phi_0)(\phi_0|H(\xi)+T+V|Q \\ &= |\phi_0)(\phi_0|VQ. \end{aligned} \tag{2.19}$$

Using these expressions, (2.15) becomes

$$\left\{E-T-(\phi_0|V|\phi_0)-\left(\phi_0\left|VQ\frac{1}{E-QHQ}QV\right|\phi_0\right)\right\}\psi_0(r_0) = 0. \tag{2.20}$$

Comparison with (2.7) gives an exact formal expression for the optical potential

$$\mathscr{V}(r_0) = (\phi_0|V|\phi_0)+\left(\phi_0\left|VQ\frac{1}{E-QHQ}QV\right|\phi_0\right). \tag{2.21}$$

The first term represents direct transitions from the incident to the outgoing channel while the second takes account of virtual nuclear excitations followed by de-excitations back into the elastic channel. The second term has singularities at the eigenvalues of QHQ, and to obtain a useful optical potential these must be smoothed by averaging over sufficiently large energy intervals.

The first term is purely real, while the second is complex, since it takes account of the nonelastic processes. Since the potential V can be expressed as a sum of the

energy-dependent constituent nucleon–nucleon interactions then the optical potential also depends on energy. Further analysis of the second term shows it to be nonlocal, so that the effective potential at any point depends on the wavefunction throughout a surrounding region of greater or lesser extent depending on the range of the nonlocality. Mathematically, the term $V(\boldsymbol{r})\psi(\boldsymbol{r})$ in the Schrödinger equation is replaced by $\int V(\boldsymbol{r},\boldsymbol{r}')\psi(\boldsymbol{r}')\,\mathrm{d}\boldsymbol{r}'$, where $V(\boldsymbol{r},\boldsymbol{r}')$ is the nonlocal potential.

Nonlocal potentials have several features that are important for optical model analyses. Firstly, to every nonlocal potential there corresponds an equivalent local potential, in the sense that they give the same asymptotic wavefunctions and hence the same phase shifts. It is thus not possible to distinguish between a local and a nonlocal potential by a phenomenological analysis. In practice optical potentials are usually taken to be purely local for practical convenience, as the use of a nonlocal potential requires the solution of an integrodifferential equation. Secondly, the local potential equivalent to an energy independent nonlocal potential depends on the energy, and the degree of energy dependence is a function of the range of the nonlocality, so that in this sense nonlocality and energy dependence are equivalent. Thus part of the energy dependence of a local potential is intrinsic, and part is due to its nonlocality. Finally, the wavefunctions corresponding to equivalent local and nonlocal potentials differ inside the nucleus, and this has implications for reaction phenomena that depend on the wavefunctions in this region. This is further discussed in § 12.

In order to proceed further in the calculation of the optical potential, it is necessary to evaluate the expression (2.21) using realistic wavefunctions and interactions. This is a very difficult and complicated problem, particularly as regards the the second term, but considerable success has been achieved by calculating the real part of the potential from the first term only and representing the imaginary part by a phenomenological potential. The remainder of this section will be devoted to a brief summary of this work, due mainly to Greenlees and his colleagues.

If $v(|\boldsymbol{r}_i-\boldsymbol{r}_j|)$ is the nuclear–nucleon interaction and $\rho_{\mathrm{m}}(\boldsymbol{r})$ the nuclear matter distribution, then the first term of (2.21) becomes

$$V(\boldsymbol{r}) = \int \rho(\boldsymbol{r}')\, v(|\boldsymbol{r}-\boldsymbol{r}'|)\,\mathrm{d}\boldsymbol{r}' \tag{2.22}$$

which is just the expression that would be written down classically. This accounts for the bulk of the real part of the optical potential, but it does omit terms corresponding to the real part of the second term in (2.21), in particular exchange terms due to the requirement of antisymmetrization. To evaluate (2.22), Greenlees *et al* (1969) used a Saxon–Woods form factor for the nuclear density and a phenomenological nucleon–nucleon interaction of the form

$$\begin{aligned} v(|\boldsymbol{r}_i-\boldsymbol{r}_j|) \equiv v(\boldsymbol{r}) = {} & v_{\mathrm{D}}(\boldsymbol{r}) + v_\tau(\boldsymbol{r})\,\boldsymbol{\tau}_i.\boldsymbol{\tau}_j + v_\sigma(\boldsymbol{r})\,\boldsymbol{\sigma}_i.\boldsymbol{\sigma}_j \\ & + v_{\sigma\tau}(\boldsymbol{r})\,(\boldsymbol{\sigma}_i.\boldsymbol{\sigma}_j)\,(\boldsymbol{\tau}_i.\boldsymbol{\tau}_j) + \{v_{\mathrm{t}}(\boldsymbol{r}) + v_{\mathrm{t}\tau}(\boldsymbol{r})\,\boldsymbol{\tau}_i.\boldsymbol{\tau}_j\}\,S_{ij} \\ & + v_{\mathrm{S}}(\boldsymbol{r})\,\hbar^{-1}\{(\boldsymbol{r}_i-\boldsymbol{r}_j)\times(\boldsymbol{P}_i-\boldsymbol{P}_j).(\boldsymbol{\sigma}_i+\boldsymbol{\sigma}_j)\} \end{aligned} \tag{2.23}$$

where S_{ij} is the tensor force operator and $\boldsymbol{\tau}_i$ the isospin operator of the ith nucleon. The real part of the optical potential may then be expressed as a sum of three terms,

$$V(\boldsymbol{r}) = V_{\mathrm{R}}(\boldsymbol{r}) + V_{\mathrm{I}}(\boldsymbol{r}) + V_{\mathrm{S}}(\boldsymbol{r}) \tag{2.24}$$

where $V_{\mathrm{R}}(\boldsymbol{r})$ is independent of spin and isospin, $V_{\mathrm{I}}(\boldsymbol{r})$ is the isospin term and $V_{\mathrm{S}}(\boldsymbol{r})$

the spin–orbit term. Defining the matter distribution $\rho_m(r)$ as the sum of the neutron and proton density distributions

$$\rho_m(r) = \rho_n(r) + \rho_p(r) \tag{2.25}$$

we obtain

$$V_R(r) = \int \rho_m(r') v_D(|r - r'|)\, dr' \tag{2.26}$$

$$V_I(r) = \tau_z \int (\rho_p(r') - \rho_n(r')) v_\tau(|r - r'|)\, dr' \tag{2.27}$$

and a rather more complicated expression for $V_S(r)$.

These expressions give the optical potential in terms of interactions and density distributions that are already known, at least approximately, and thus remove many of the uncertainties of a purely phenomenological analysis. In practice it is usual to treat the radius and diffuseness of the nuclear matter distribution as adjustable parameters in order that they may be determined by comparison with experimental data.

In their calculations, Greenlees *et al* (1968, 1970a,b) used a Yukawa form for $v_D(r)$ and adjusted its strength and range to the two-body data. The imaginary part of the potential cannot easily be calculated, so they used a purely phenomenological expression. They were able to fit their calculations to experimental data on

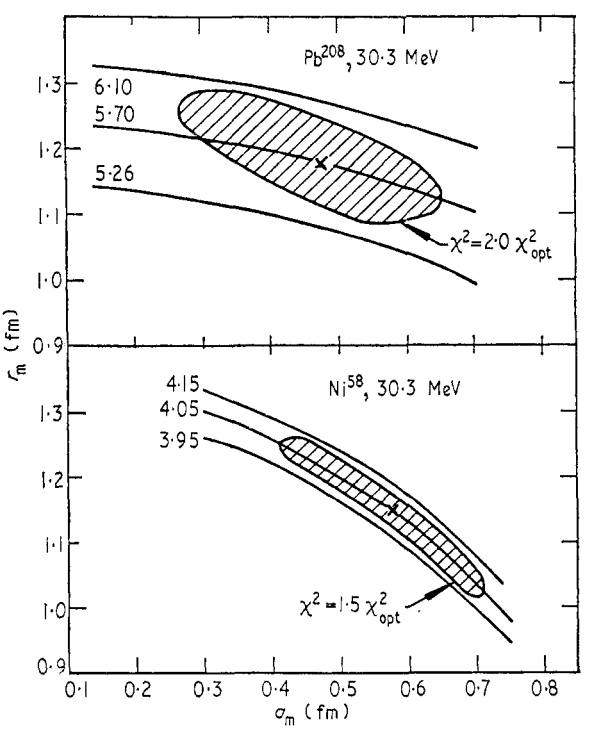

Figure 3. Contours of best fit χ^2 values for variations of matter radius (r_m) and diffuseness (a_m) parameters. The crosses represent the best-fit points. The shaded area encompasses a region within which the fits are visibly indistinguishable. Lines of constant root mean square matter radius $\langle r^2 \rangle_m^{1/2}$, denoted by values in fermis, are seen to run nearly parallel to the sides of the shaded areas. From Greenlees *et al* (1968).

elastic scattering of 30 MeV protons by several medium and heavy nuclei, using matter distributions in accord with those found in other investigations. An important result of this analysis is that the elastic scattering data fixes the root mean square radius of the real part of the optical potential and its volume integral per nucleon much more accurately than the three parameters of the corresponding form factor. The volume integral per nucleon is found to be independent of energy and the nuclear symmetry parameter $(N-Z)/A$. These results are illustrated in figures 3 and 4.

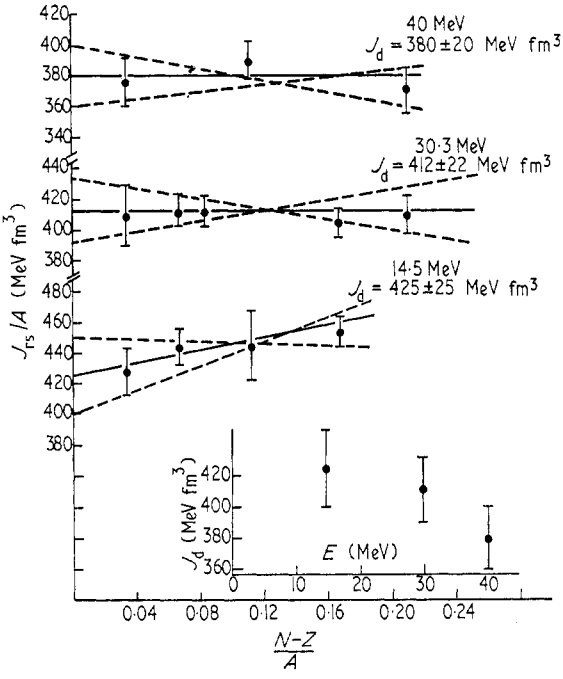

Figure 4. Variation of J_{rs}/A, the volume integral per nucleon, with $(N-Z)/A$ for the potentials found by analyses of the elastic scattering of 14·5, 30·3 and 40 MeV protons by nuclei. The energy variation of the values for $N = Z$ nuclei is shown in the inset. From Greenlees *et al* (1968).

The accuracy of the matter distribution depends on the extent to which the terms not included in (2.3) are indeed small. The first calculations of Greenlees *et al* (1968) gave matter distributions with too large a radius, but subsequent work (Greenlees *et al* 1970a,b) gave more acceptable values. A detailed evaluation of the more important additional terms is necessary before reliable matter distributions can be obtained. Encouraging progress in this respect has been made by Owen and Satchler (1970) and by Kidwai and Rook (1971).

The reformulated optical model, as it is called, has been used in several analyses of neutron and proton elastic scattering data, and gives results comparable in quality with those obtained with the purely phenomenological optical model (Pyle and Greenlees 1969, Boyd *et al* 1970, Woolam *et al* 1970). In some cases, however, particularly at back angles, the fits are not yet adequate, and it is clear that more work needs to be done on the higher-order correction terms to (2.22). Recent studies of the interactions of light nuclei using the resonating group method suggest

how this might be done. Thus Tang (1969) has shown that when antisymmetrization is taken into account the wavefunction describing the interaction between two light nuclei satisfies the equation

$$\nabla^2\psi(\boldsymbol{r})+\frac{2m}{\hbar^2}(E-V_{\mathrm{R}}(r)-V_{\mathrm{C}}(r))\psi(\boldsymbol{r})=\int K(\boldsymbol{r},\boldsymbol{r}')\psi(\boldsymbol{r}')\,\mathrm{d}\boldsymbol{r}' \tag{2.28}$$

where $V_{\mathrm{R}}(r)$ is the direct potential obtained by folding the matter distribution and the nucleon–nucleon interaction, and $K(\boldsymbol{r},\boldsymbol{r}')$ is a nonlocal kernel of the form

$$K(\boldsymbol{r},\boldsymbol{r}')=g_1(r,r')\exp\{-\beta_1(\boldsymbol{r}-\boldsymbol{r}')^2\}+g_2(r,r')\exp\{-\beta_2(\boldsymbol{r}+\boldsymbol{r}')^2\} \tag{2.29}$$

where β_1 and β_2 are related to the ranges of the nonlocalities. The first of these terms is a nonlocality of the type already used by Perey and Buck (1962) in their analysis of neutron scattering, while the second gives the exchange contributions and is particularly important at back angles. It is likely that similar terms are also present in the full expression for the optical potentials for heavier nuclei. Thus inclusion of the latter term in the optical potential could improve the fits in the backward direction for the differential cross section for 30 MeV protons on ^{58}Ni, and possibly also the back angle data for α particle scattering, though in this case other effects may also be present (see § 9) (Greenlees and Tang 1971).

In all these calculations of the optical potential, the real part obtained from a folding procedure is supplemented by a phenomenological imaginary potential. Many attempts have, however, been made to calculate the imaginary potential; indeed the earliest semichemical model already gave a simple expression in terms of the velocity of the particle and its absorption coefficient K in nuclear matter,

$$W=v\hbar K/2 \tag{2.30}$$

where

$$K=\frac{3A\sigma}{4\pi R^2} \tag{2.31}$$

R being the nuclear radius and σ the mean cross section for nuclear collisions

$$\sigma=\{Z\sigma_{\mathrm{np}}\alpha_{\mathrm{np}}+(A-Z)\sigma_{\mathrm{nn}}\alpha_{\mathrm{nn}}\}/A. \tag{2.32}$$

The coefficients α_{np} and α_{nn} allow for the reduction in cross section due to the Pauli principle, and have been evaluated semiclassically by Goldberger (1948).

These calculations of the imaginary potential have been improved by introducing more exact expressions for the nucleon–nucleon interaction and more sophisticated ways of allowing for the Pauli principle (Greenlees *et al* 1968, Afnan and Tang 1970). This confirms two important features of the phenomenological potential, namely that it increases with increasing energy and that its radial extent is substantially greater than that of the real part of the potential. The final form of the potential depends in rather a complicated way on the energy variations of the contributing interactions and on the inhibiting effect of the Pauli principle. There are still discrepancies between the calculated and phenomenological potentials, which may be due to nonlocal effects arising from antisymmetrization. Further work is thus necessary to define the form of the imaginary part of the potential and its variation with energy. The remaining uncertainty in the imaginary potential fortunately does not affect the work on the real part of the potential, since the fit to experimental data is quite insensitive to the form chosen, provided its parameters are optimized.

3. Nuclear single-particle states

Any potential of sufficient depth has a series of bound states, and their ordering and specification by the total, orbital and spin quantum numbers is familiar from the shell model. The energies of these states may easily be found experimentally using one-nucleon transfer reactions for nuclei near closed shells that often have low-lying single-particle states of high purity. Even for nuclei away from closed shells where the single-particle states are split into many fragments by the residual interactions it is still possible to define an equivalent single-particle energy

$$\bar{E} = \sum_i g_i E_i \tag{3.1}$$

where the g_i are the weights (spectroscopic factors) of the fragments of energies E_i. The cross section for a one-nucleon transfer reaction to such a state is given by

$$\frac{\mathrm{d}\sigma}{\mathrm{d}\Omega} = \mathscr{S} F(E, \theta) \tag{3.2}$$

where $\mathscr{S}$ is the spectroscopic factor that depends only on the structures of the initial and residual nuclei and all the energy and angular dependence is contained in the reaction factor $F(E, \theta)$, which may be calculated by the distorted wave theory. These calculations are now so well understood and calibrated that providing the direct nucleon transfer reaction is the dominant mode and the final state is largely single particle, the absolute cross section, and hence the spectroscopic factor, can be determined to within about 20%, thus providing a powerful method of obtaining the energies and strengths of single-particle states. Neutron single-particle states are most conveniently studied by the (d, p) and (p, d) reactions for the unfilled and filled levels respectively and the proton states by the (h, d) and (d, h) reactions, as in the (d, n) and (n, d) reactions it is difficult to determine the neutron energies with sufficient precision.

Single particle states may also be studied by nucleon knockout reactions, particularly (p, 2p), and although the corresponding energy measurements are usually less accurate than for the nucleon transfer reactions they do enable rather deeply lying states to be investigated. Once the energies of the single-particle states are known the depth of the corresponding potential may easily be determined, providing a suitable form factor is assumed. It is usual to take a potential of the form

$$V(r) = Vf(r) + V_{\mathrm{S}} f_{\mathrm{S}}(r) \tag{3.3}$$

with the form factors given by (2.1) and (2.2). For charged particles the electrostatic potential due to a uniformly charged sphere is added to (3.3). It is convenient to begin by describing the method of solution in the absence of a spin–orbit term. If this potential is inserted in the Schrödinger equation and the wavefunction expanded as a product of angular and radial functions

$$\Psi(\boldsymbol{r}) = \sum_L \frac{u_L(r)}{r} \mathrm{i}^L P_L(\cos\theta) \tag{3.4}$$

the usual multiplication from the left by $P_{L'}(\cos\theta)$ and integration over the angular coordinates gives the radial wave equation

$$\frac{\mathrm{d}^2 u_{NL}(r)}{\mathrm{d}r^2} + \left(\frac{2m}{\hbar^2}(E - V(r)) - \frac{L(L+1)}{r^2}\right) u_{NL}(r) = 0. \tag{3.5}$$

Since the nuclear potential falls rapidly to zero the asymptotic solution to this wave

equation may be obtained by solving analytically the equation without the term $V(r)$. This external solution may then be matched to the solution in the internal region, and the required bound state is defined by the condition that the interior and exterior solutions match smoothly. Since the energy is not known, an iterative method has to be used. For each value of the orbital angular quantum number L there are several internal solutions, with different numbers of nodes, that can be matched to the exterior solution. These correspond to states of different principal quantum number N, which is accordingly required to specify the bound states. The whole calculation can be carried out electronically and the convergence is rapid (Hodgson 1963).

In practice the potential contains a spin–orbit term $V_S f_S(r)$ and this gives two radial wave equations with total angular momenta $J = L \pm \frac{1}{2}$, corresponding to the two spin orientations. Each of these equations may be solved in the way already described. The energies of the two components of a $J = L \pm \frac{1}{2}$ pair, for example of the $1p_{1/2}$ and $1p_{3/2}$ states, then suffice to fix both V and V_S. The potential is thus determined for particular values of N and L, unlike the optical potential for free particles which is assumed to be the same for all N and L. The study of bound single-particle states can thus give information on the state dependence of the potential.

Many studies of single-particle states in nuclei have now been made, particularly in nuclei with closed shells plus or minus one nucleon, for then the single-particle states are particularly pure. In the case of ^{208}Pb, for example, there are four nuclei that may be found by adding or subtracting a nucleon, and in these at least 22 strongly marked single-particle states may be identified. If the parameters of the potential (3.3) are then adjusted to optimize the overall fit to these states, the usefulness of the model can be evaluated. This has been done by Rost (1968) and some of his results are shown in figure 5. The overall fit to the data is as good as can be expected with such a simple model. Similar calculations have been made by Batty and Greenlees (1969).

These single-particle potentials can be used to calculate the wavefunctions, and hence the matter and charge distributions for the particles in the observed levels, and if it is assumed that the same potential applies to the lower-lying particles as well the distributions for the whole nucleus can be obtained. The resulting charge distributions have been found to account very well for the elastic scattering of 175 and 250 MeV electrons by ^{208}Pb, and this constitutes a useful check on the model (Elton 1968).

If these single-particle states are studied throughout the periodic table, the variation of their binding energies with neutron and proton numbers may be studied. An overall picture may be obtained by calculating the energies of all the single-particle states in the potential (3.3), with all the parameters fixed, except the radius which is allowed to depend on A. The result of such a calculation is shown in figure 6. The grouping of the studies into bands characteristic of the shell model is immediately evident.

Detailed studies of bound single-particle states are made in two ways; firstly by examining as many states as possible in the same nucleus as in the work on ^{208}Pb already mentioned, and secondly by following particular states from one nucleus to the next across the periodic table.

Several analyses of the former type have been made for light and medium weight nuclei, as well as for ^{208}Pb. Thus Brown *et al* (1963) studied the single-particle

states in Ni and Pb and found that the calculated levels tended to be rather more widely spaced than the observed levels. This can be accounted for if the potential depends on either the state or the energy of the particle concerned. They chose the latter alternative, and found that if this energy dependence is expressed in terms of effective mass, then m^*/m is greater than unity. This is in contrast to the situation for positive energies, where the energy dependence corresponds to an effective mass around $0{\cdot}7m$.

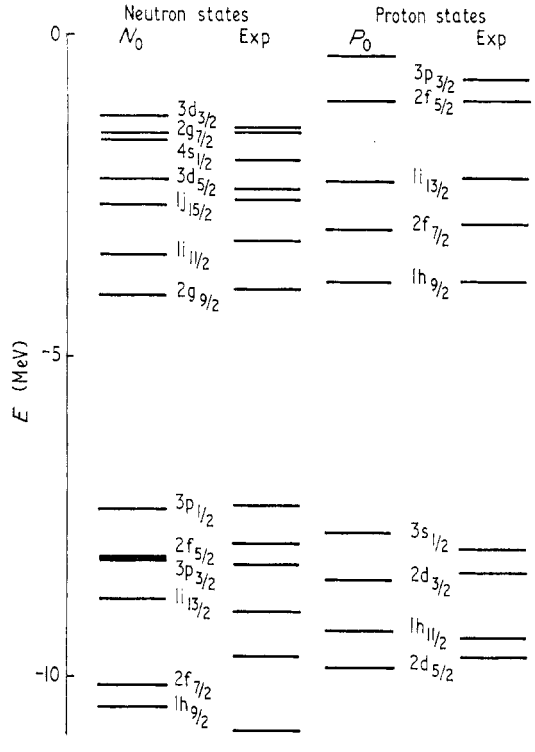

Figure 5. Comparison between single-particle and single-hole states for ^{208}Pb and the eigenvalues of bound state potentials. The parameters of the potentials are for neutrons $V = 40{\cdot}6$, $r_u = 1{\cdot}347$, $V_s = 14{\cdot}1$, $r_s = 1{\cdot}28$ and for protons $V = 58{\cdot}7$, $r_u = 1{\cdot}275$, $V_s = 11{\cdot}5$, $r_s = 0{\cdot}932$. All surface diffuseness parameters are fixed at 0·7. From Rost (1968).

The single-particle states have been studied for a range of nuclei by Cohen (1965) and he found that it is necessary to allow the potential to depend on the nuclear symmetry parameter $(N-Z)/A$, together with an energy dependence equivalent to an effective mass of about $1{\cdot}3m$. The large number of measurements of nucleon transfer reactions made during the last few years enables this analysis to be extended in a more precise way to a larger range of nuclei. For such work it is necessary to take into account the implications of the isospin dependence of the potential. A proton stripping reaction can excite both $T_>$ and $T_<$ states, while the condition that $T \geqslant T_Z$ implies that the neutron stripping reaction can excite only $T_>$ states, and conversely for pickup reactions. If the nucleon optical potential contains an isospin term of the form

$$V_1(r) = 4/f(r)\frac{V_1}{A}\boldsymbol{t}.\boldsymbol{T}\frac{4V_1}{A}\boldsymbol{t}.\boldsymbol{T}f(r) \tag{3.6}$$

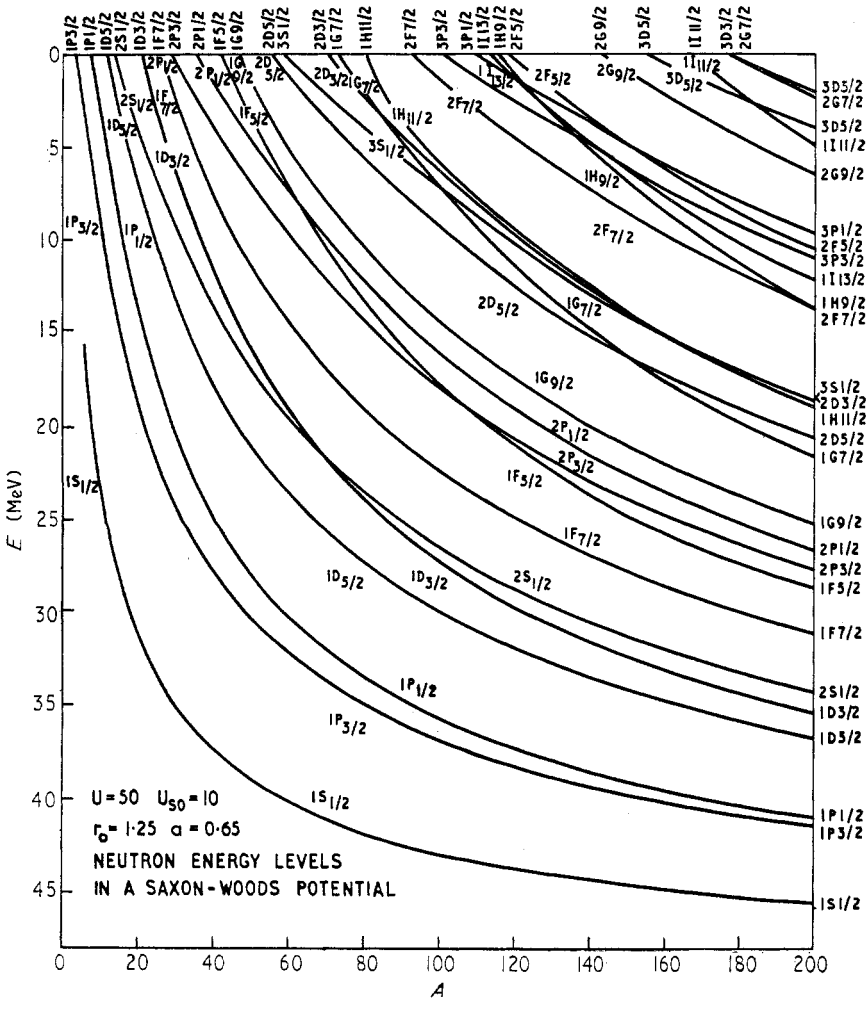

Figure 6. Single-particle states (neutron energy levels) in a Saxon–Woods potential.

where t and T are the isospins of the incident nucleon and target nucleus respectively, the resulting expressions for the potentials are, for stripping reactions,

$$\left.\begin{aligned} V_{\mathrm{N}}^{>} &= V_0 - V_1(N-Z)/A \\ V_{\mathrm{P}}^{<} &= V_0 + V_1(N-Z+2)/A + \beta Z/A^{1/3} \\ V_{\mathrm{P}}^{>} &= V_0 - V_1(N-Z)/A \end{aligned}\right\} \tag{3.7}$$

and for pickup reactions

$$\left.\begin{aligned} V_{\mathrm{N}}^{<} &= V_0 - V_1(N-Z-1)/A \\ V_{\mathrm{P}}^{>} &= V_0 + V_1(N-Z+3)/A + \beta(Z-1)/A^{1/3} \\ V_{\mathrm{N}}^{>} &= V_0 + V_1(N-Z+3)/A \end{aligned}\right\} \tag{3.8}$$

where N, Z and A refer to the target nucleus. The extra term $0{\cdot}4Z/A^{1/3}$ has been added to the proton potentials for the reasons described in §6. As this term is

relatively small, it is sufficiently accurate to assume that it has the same form factor as the major part of the potential, so the correction then appears in the above expression for potential depths.

The bound-state potentials differ from the free state ones in that once the form factor and potential depth are specified, the energy of a particular quantum state is determined. If the potential is state dependent it is thus superfluous to allow the potential depth V to depend on E as well as on A, and a choice has to be made. An A dependence is preferable to the more usual energy dependence since it is indicated phenomenologically, and since this choice also absorbs any inadequacies in the assumed A dependence of the nuclear radius (usually $R = r_0 A^{1/3}$). Thus in the above expressions V_0 is allowed to depend on A but not on E.

Analysis of the available data on single-particle states yields consistent values of V_0 and V_1 with a linear dependence of V_0 on A. In the case of 2S hole states in medium weight nuclei, for example (Millener and Hodgson 1971),

$$\begin{aligned} V_0 &= 59 - 0{\cdot}2A \\ V_1 &= 37 \end{aligned} \tag{3.9}$$

where V_0 and V_1 are in MeV. Similar values are obtained for the states of higher orbital angular momentum, and enable the state dependence of the potential to be investigated.

Some investigations of single-particle states have been made using nonlocal potentials (Meldner 1969). As shown in the previous section, the potential is partly local and partly nonlocal, and that for bound states is likely to be more strongly nonlocal than the potential for elastic scattering since the potential depends on an overlap of wavefunctions, and this is greater between bound states than between a bound state and a scattering state. It has however been found by Grimm *et al* (1971) that it is not possible to account for all the features of bound states using a purely nonlocal potential, and since it is impracticable to use a potential with both local and nonlocal components it is simpler to use one that is purely local, remembering that part of it has a nonlocal origin and hence gives rise to a significantly different wavefunction (see § 12).

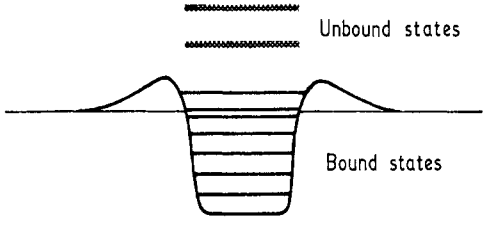

Figure 7. Bound and unbound states of a potential well.

The nucleon–nucleus potential has unbound states as well as bound states (see figure 7); these are sometimes referred to as bound states embedded in the continuum. The energies of these states may be calculated in a similar way to the corresponding bound states, except that now the interior wavefunctions are matched to the scattering wavefunctions that are solutions of the appropriate Schrödinger radial wave equation. The resonances occur at energies for which the phase shift η passes through $\pi/2$ and the rate $\mathrm{d}\eta/\mathrm{d}E$ at which it does so is proportional to its width

and inversely proportional to its lifetime. The resonances are sharp and long-lived at low energies and become broader and shorter-lived as the energy increases. If reaction channels are open the resonances are correspondingly broadened, and this may be taken into account by allowing the potential to become complex.

These unbound states may be investigated experimentally in several ways, in particular by elastic scattering and nucleon-transfer reactions. For light nuclei at low energies the reaction channels are closed and the unbound states are sharp enough to be clearly visible on the elastic scattering excitation function, particularly at backward angles. Apart from these resonances, the cross section is frequently purely Rutherford, so the cross section may easily be analysed as a superposition of a Coulomb and a Breit–Wigner amplitude, and hence the energy, spin and width of the unbound state determined. At higher energies the nuclear scattering becomes significant, and the corresponding scattering amplitude may easily be calculated from an optical model potential adjusted to the data in the regions away from resonances. Comparison between the measured and calculated width gives immediately the single-particle strength of the state. Thus, for example, a $d_{5/2}$ resonance occurs at 1·75 MeV in the elastic scattering of protons by carbon. If the depth of a potential with standard form factors is adjusted to give a $d_{5/2}$ resonance at this energy the corresponding width is 56 keV. Since the measured width is 61 keV the state is essentially a pure single-particle one (Schiffer 1963).

Unbound single-particle states can also be studied by nucleon transfer reactions. The lifetime of the state is usually much greater than the reaction time so the reaction is unaffected by its subsequent decay. The angular distributions are characteristic of the orbital angular momentum transfer, and the absolute cross sections give the spectroscopic factor and parity of the single-particle state, in just the same way as in nucleon transfer reactions to bound states.

The calculation of the cross section of direct reactions to unbound states may be made with the same distorted wave formalism as for bound states except that the wavefunction of the captured particle has the oscillatory tail at large distances characteristic of a scattering state. Inside the nucleus the wavefunction at the resonance energy is very similar to that of a bound state. These wavefunctions may be calculated by solving the radial wave equation at the resonance energy or by using the Gamow pole functions (Bang and Zimanyi 1969). The oscillatory tail of these unbound state wavefunctions gives rise to convergence difficulties in the overlap integral for the reaction matrix elements. There are large, alternatively positive and negative, contributions from outside the reaction region and, though these eventually cancel, small numerical errors can have a large effect on the final result. In practice the integration is carried out numerically as far as an external cut-off radius, chosen so that the contribution from the region still farther out is negligible. For direct reactions to bound states it is sufficient to integrate to a few fermis beyond the nuclear surface, but for unbound states adequate convergence is often not attained by integrating out to 100 fm or more (Fortune *et al* 1969, Youngblood *et al* 1970). Several attempts have been made to improve the convergence of the integral by the application of a convergence factor (Huby and Mines 1965) and by altering the path of integration (Fortune and Vincent 1969). More recently, Huby (1970) has proposed the use of 'pseudobound' wavefunctions, obtained as unbound eigenvalues of the appropriate Saxon–Woods potential, the small oscillations at large distances being cut off exponentially near the first node outside the nucleus. Huby justifies this prescription by Weinberg's quasiparticle

formalism, and the results are found to be insensitive to the precise details of the cut-off (Cole *et al* 1970). The spectroscopic factors found in this way are consistent with those obtained for the widths of the corresponding resonances excited by elastic scattering. It is thus now possible to analyse transitions to unbound states just as easily as those to bound states.

The optical potentials describing the interaction of composite particles with nuclei also have unbound states, and although they are too broad to be observable in most circumstances, it is possible that they could be found at low energies in light nuclei. A possible indication of the presence of such states is found in the α particle transfer reactions in medium weight nuclei studied by Faraggi *et al* (1971). Figure 8

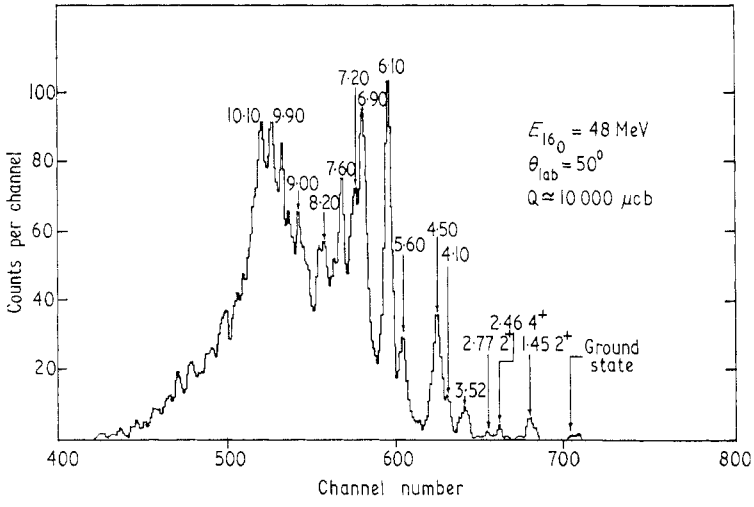

Figure 8. Energy spectrum of the outgoing particles in the reaction $^{54}Fe(^{16}O, ^{12}C)^{58}Ni$ showing the peaks ascribed to α particle resonant states. From Faraggi *et al* (1971).

shows the energy spectrum of the outgoing particles in the $^{54}Fe(^{16}O, ^{12}C)^{58}Ni$ reaction, and there are several prominent peaks at energies where the level density in the residual nucleus is so high that a smooth Maxwellian energy distribution is expected. Similar results were obtained for several medium weight nuclei. Lane (1971 private communication) has suggested that these observations could be explained if the α particle was first captured into a resonant or unbound state in an α particle optical potential and preliminary calculations (Dudek and Hodgson 1972) show that the observed density of such states is in accord with this model. The states are grouped into bands, each corresponding to a particular number of oscillator quanta, and alternate bands are composed of states with all odd J and all even J. It will be a critical test of this model to confirm this prediction, and this can be done in principle by comparing the experimental angular distributions with distorted wave calculations in the usual way.

4. Nuclear reactions

In order to define the conditions under which the optical model may be used to calculate nuclear interaction cross sections it is necessary to consider all the types of reaction that take place. This will be done for the special case of protons but the discussion is applicable to other particles as well.

A proton incident on a nucleus can undergo either a direct scattering or reaction in a time of the order of the transit time, or it can be captured to form a compound nucleus. The direct processes are (shape) elastic scattering, inelastic scattering and the whole range of charge-exchange, knockout and nucleon-transfer reactions. If the proton is captured to form the compound nucleus a complicated excitation

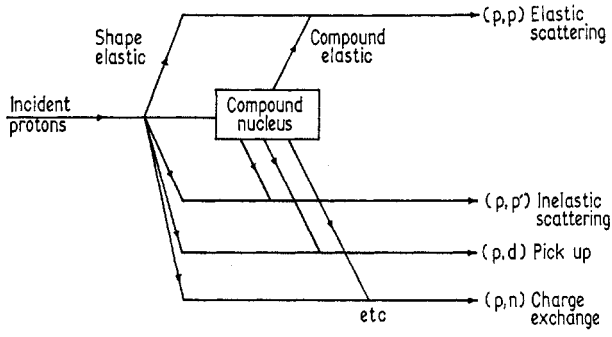

Figure 9. Direct and compound nucleus processes in nuclear reactions.

process takes place and, after a long time on the nuclear scale, it de-excites by emission of particles and eventually β and γ rays. The particles can be emitted into all the open reaction channels, including the elastic channel, and thus all cross sections have both a direct and a compound nucleus component. This is illustrated schematically in figure 9.

The cross sections of the direct process vary smoothly with energy, while those of the compound nucleus processes show rapid fluctuations over energy intervals that may be as small as a few electron volts or less. This difference arises from the

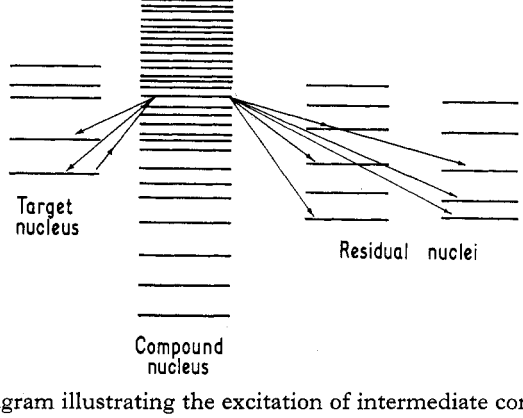

Figure 10. Energy diagram illustrating the excitation of intermediate compound nucleus states in a nuclear reaction.

characteristics of the two processes. Direct reactions proceed directly from the initial to the final state and so the cross section depends on a matrix element expressible in terms of the initial and final wavefunctions and the interaction hamiltonian; since these vary smoothly with energy so does the cross section itself. Compound nucleus reactions, on the other hand, proceed through a very large number of complicated intermediate states. The density of levels in the compound nucleus is very high, and so, as indicated schematically in figure 10, a very small change in

the incident energy suffices to alter completely the intermediate states, and hence the cross section.

This difference between the energy dependence of direct and compound nucleus reactions may also be seen as a consequence of the time they take, making use of the uncertainty relation between energy and time, $\Delta E \Delta t \geqslant h$. Thus a direct process, taking say 10^{-22} s, can show appreciable energy variation only for $\Delta E \simeq 10$ MeV, while a compound nucleus process, taking say 10^{-16} s, can show energy variation for $\Delta E \approx 10^{-5}$ MeV. The mean width of the fluctuations depends on the incident energy and the target nucleus, decreasing both with energy and with nuclear mass. For some light nuclei at low energies the level density is such that

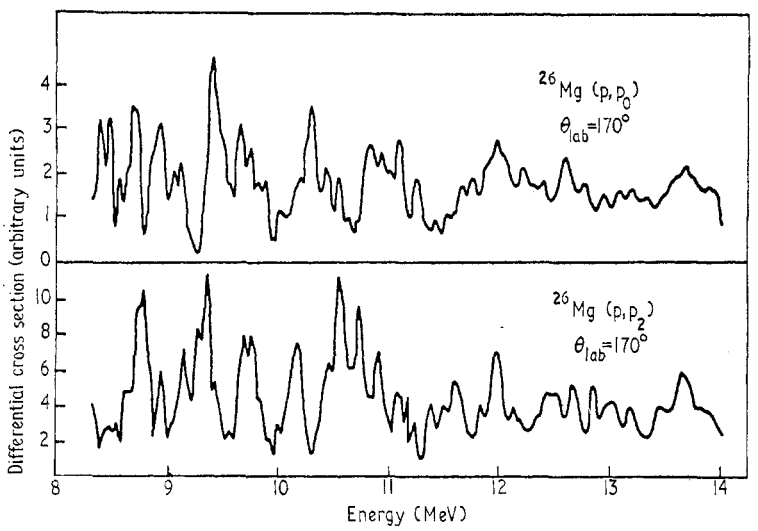

Figure 11. Excitation functions for the reactions ^{26}Mg(p, p_0) and ^{26}Mg(p, p_2) showing fluctuations. The amplitude of the fluctuations decreases with increasing energy due to the rising contribution of direct processes to the reactions. From Häusser *et al* (1964).

accurate and painstaking measurements are able to show the rapid fluctuations of the cross section with incident energy. Two examples of such cross sections are shown in figure 11 which also illustrates the gradual decline in the amplitude of the fluctuations as the relative proportion of compound nucleus cross section diminishes.

In order to analyse such cross sections these two processes must be disentangled. The direct contribution to the elastic scattering may be calculated from the optical potential as described in § 5. The compound nucleus cross section is far too complicated to calculate in detail, as it depends on the properties of all the myriad compound states. It is however possible to analyse the overall statistical features of the fluctuating cross sections and hence to obtain the ratio of direct to compound contributions. A simple analysis is possible if the cross sections are averaged over energy intervals greater than the mean width of the fluctuations. The energy-averaged compound nucleus cross sections can be calculated as described in § 11, and the analysis given later in this section shows that the observed cross section is simply the sum of the direct cross section and the energy-averaged compound nucleus cross section. Thus the compound nucleus component may be subtracted from the measured cross section to give the direct (shape elastic) cross section, and this may be analysed as described in § 5.

At higher energies the compound nucleus contribution to a particular channel is frequently negligible, as the number of channels open to the decay of the compound nucleus increases extremely rapidly with energy. In other cases the compound nucleus contribution is appreciable and must be subtracted before an optical model analysis can be made. It is thus essential to understand the relation of the direct and compound processes before commencing an optical model analysis. This may be done by using the theory of nuclear reactions to relate the real (fluctuating) cross sections to the energy-averaged cross sections. For simplicity it is convenient to consider only the S wave ($L = 0$) neutron channel; this gives the essential physics and the results may easily be extended to the other channels.

The elastic scattering is completely described by the (energy dependent) matrix element S, and the elastic, reaction and total cross sections are then given by

$$\left.\begin{aligned}\sigma_{\mathrm{E}} &= (\pi/k^2)|1-S|^2\\ \sigma_{\mathrm{R}} &= (\pi/k^2)(1-|S|^2)\\ \sigma_{\mathrm{T}} &= (2\pi/k^2)(1-\mathrm{Re}\,S).\end{aligned}\right\} \tag{4.1}$$

The matrix element S and the corresponding cross sections fluctuate rapidly with energy. The energy-averaged quantities may similarly be described by an average matrix element $\langle S\rangle$, where the angular brackets represent averaging over an energy interval larger than the mean width of the underlying resonances. Thus

$$\left.\begin{aligned}\hat{\sigma}_{\mathrm{E}} &= (\pi/k^2)|1-\langle S\rangle|^2\\ \hat{\sigma}_{\mathrm{R}} &= (\pi/k^2)(1-|\langle S\rangle|^2)\\ \hat{\sigma}_{\mathrm{T}} &= (2\pi/k^2)(1-\mathrm{Re}\langle S\rangle).\end{aligned}\right\} \tag{4.2}$$

These quantities may be related by expressing the matrix element S as the sum of an average and a fluctuating component

$$S = \langle S\rangle + \hat{S}. \tag{4.3}$$

Then substituting in (4.1) and carrying out the energy-averaging

$$\left.\begin{aligned}\sigma_{\mathrm{E}} &= \hat{\sigma}_{\mathrm{E}} + \sigma_{\mathrm{F}}\\ \sigma_{\mathrm{R}} &= \hat{\sigma}_{\mathrm{R}} - \sigma_{\mathrm{F}}\\ \sigma_{\mathrm{T}} &= \hat{\sigma}_{\mathrm{T}}\end{aligned}\right\} \tag{4.4}$$

where the fluctuating cross section σ_{F} is defined by

$$\sigma_{\mathrm{F}} = (\pi/k^2)(\langle|S|^2\rangle - |\langle S\rangle|^2). \tag{4.5}$$

To investigate this fluctuating component it is necessary to make use of the expression for the S matrix element in terms of a phase shift that varies smoothly with energy and a sum over the underlying compound nucleus resonances

$$S = \mathrm{e}^{2\mathrm{i}\delta}\left(1 - \sum_s \frac{\mathrm{i}\Gamma_{\mathrm{n}}^s}{E - E_s + \mathrm{i}\Gamma^s/2}\right) \tag{4.6}$$

and hence

$$\langle S\rangle = \mathrm{e}^{2\mathrm{i}\delta}\left(1 - \frac{\pi\bar{\Gamma}_{\mathrm{n}}}{D}\right) \tag{4.7}$$

where $\bar{\Gamma}_n$ is the mean neutron width and D the mean level separation. The compound nucleus contribution to the cross section can be calculated from the Breit–Wigner resonance formalism, giving

$$\langle\sigma_{CN}\rangle = \left(\frac{\pi}{K^2}\right)\left(\frac{2\pi\bar{\Gamma}_n}{D}\right). \tag{4.8}$$

Then putting (4.7) in (4.2), neglecting terms in $(\bar{\Gamma}/D)^2$ and using (4.5) gives

$$\langle\sigma_R\rangle = \langle\sigma_{CN}\rangle - \sigma_F. \tag{4.9}$$

Since

$$\langle\sigma_{CN}\rangle = \langle\sigma_R\rangle + \langle\sigma_{CE}\rangle \tag{4.10}$$

the fluctuating component is identified as the compound elastic contribution to the cross section and this applies to the differential as well as to integrated cross sections. It is thus possible to analyse a cross section with direct and compound components by evaluating them independently and then simply adding the results. Some examples of such analyses are given in § 11.

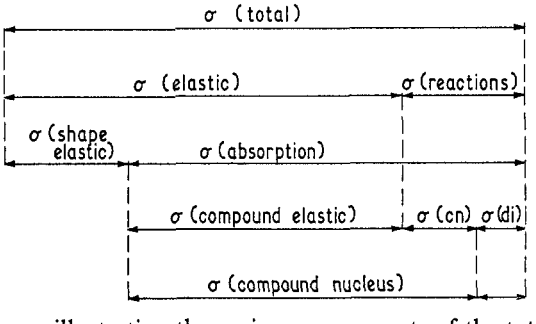

Figure 12. Diagram illustrating the various components of the total cross section.

The various contributions to the total cross section are shown schematically in figure 12.

5. Optical model calculations

The shape elastic cross section may be calculated from the optical potential $V(r)$ by solving the Schrödinger wave equation

$$\nabla^2\Psi + (2m/\hbar^2)(E - V(r))\Psi = 0 \tag{5.1}$$

subject to the boundary conditions of incident plane wave and an outgoing scattered wave

$$\Psi \sim e^{ikz} + (1/r)\, e^{ikr} f(\theta). \tag{5.2}$$

It is usual to assume the optical potential is spherically symmetrical so that the wavefunction can be expanded in Legendre polynomials

$$\Psi = \sum_L \frac{u_L(r)}{r} i^L P_L(\cos\theta) \tag{5.3}$$

where L is the orbital angular momentum quantum number. Substituting this in

(5.1) and carrying out the angular integration gives the radial wave equation for the Lth partial wave

$$\frac{\mathrm{d}^2 u_L(r)}{\mathrm{d}r^2} + \left(\frac{2m}{\hbar^2}(E - V(r)) + \frac{L(L+1)}{r^2}\right) u_L(r) = 0. \tag{5.4}$$

This equation may be solved for any given $V(r)$ by integrating step by step outwards from the origin using the appropriate numerical technique. This gives the wavefunction outside the nuclear field, and comparison with the corresponding wavefunction in the absence of the nuclear field immediately yields the phase shift δ_L and hence the matrix element

$$S_L = \mathrm{e}^{2\mathrm{i}\delta_L}. \tag{5.5}$$

This can be done for all partial waves and hence the differential cross section

$$\frac{\mathrm{d}\sigma}{\mathrm{d}\Omega} = |f(\theta)|^2 \tag{5.6}$$

where

$$f(\theta) = (1/2\mathrm{i}k) \sum_{L=0}^{\infty} (2L+1)(S_L - 1) P_L(\cos\theta). \tag{5.7}$$

This outline of the calculation refers to neutral spinless particles, and may easily be generalized to charged particles with spin (Hodgson 1963). In the case of charged incident particles the Coulomb (electrostatic) field of the nucleus is added to the optical potential and allowance is made for the particular analytic properties of the Coulomb wavefunctions in the asymptotic region. If the particle has spin the total wavefunction is expanded as a product of spatial and spin wavefunctions, and the operator $\boldsymbol{L}.\boldsymbol{\sigma}$ in the spin dependent part of potential (2.2) splits each radial wave equation into $(2S+1)$ components corresponding to the possible values of $\boldsymbol{J} = \boldsymbol{L} + \boldsymbol{S}$. These may be solved in a similar way and the resulting S matrix elements combined to give not only the differential and total cross sections but also the polarization of the scattered particles as well.

The formalism may also be applied to calculate the change in polarization when the incident particles are polarized. This is frequently used in connection with the scattering of deuterons, due to the complexity of the corresponding polarization phenomena.

When realistic potentials are used, the calculations must be carried out numerically and may easily be programmed for an electronic computer. These computer programs enable the differential cross sections, polarizations and other measurable quantities to be calculated for any specified potential. Usually, however, one needs to find the potential that gives the best fit to a particular set of data. The calculation cannot be reversed, essentially because of the loss of information that occurs when the complex scattering amplitude is squared to give the cross section, so the only way to proceed is to adjust the parameters of the potential to optimize the fit to the data. Many automatic techniques have been developed to do this and they have been incorporated in the optical model programs so that the whole calculation may be done at once. It frequently happens that there are several potentials that give equally good fits to the data. Examples of these ambiguities, together with ways of overcoming them, are given in the following sections.

6. The elastic scattering of nucleons

In this and the three subsequent sections the optical model is applied to the analysis of elastic scattering cross sections and polarizations in conditions where the compound elastic contribution either is negligible or has been evaluated and subtracted by the methods of § 11. The scattering may then be calculated directly from the optical potential by the methods of § 5. In practice it is required to obtain the potential from the experimental data, and this may be done by systematically varying the parameters of the optical potential to optimize the overall fit to the data, using appropriate computer programs.

Many different expressions have been used for the nucleon optical potential. All have a real central term of Saxon–Woods or similar form, and an imaginary volume or surface-peaked term. To account for polarization data a spin–orbit term of the form (2.2) familiar from shell model studies is added. The precision of optical model analyses makes it possible to study the presence of small terms in the potential, and among these the isospin term has received much attention. Some work has also been done to investigate the possibility of terms depending on the spin and magnetic moment of the target nucleus. Apart from these small terms, the standard optical model potential may be written in the form

$$V(r) = V_C(r) + Vf_1(r) + \mathrm{i}(W_v f_2(r) + W_s g(r)) + \left(\frac{\hbar}{m_\pi c}\right)^2 \frac{V_S}{r}\frac{\mathrm{d}f_3(r)}{\mathrm{d}r} \boldsymbol{L}.\boldsymbol{\sigma} \qquad (6.1)$$

where $V_C(r)$ is the electrostatic potential (for protons only) which may be taken without appreciable error as that due to a uniformly charged sphere with the same radius as the real part of the potential, the $f_i(r)$ are Saxon–Woods form factors that may have different radius and diffuseness parameters, $g(r)$ is a surface-peaked form factor usually taken to be the radial derivative of a Saxon–Woods form factor, and W_v and W_s are the volume and surface absorption potentials.

The earliest analyses used square well potentials but these were replaced by the physically more realistic rounded wells as soon as electronic computers made it practicable to solve the corresponding radial wave equations numerically. Accurate analyses of differential cross sections and polarizations for the elastic scattering of 183 MeV protons by a range of nuclei soon showed that it is necessary to allow the radius parameter of the imaginary part of the potential to exceed that of the real part by about 20 % (Hodgson 1961, Johansson *et al* 1961), and that the fit is also improved by allowing the corresponding diffuseness parameters to differ as well (Satchler and Haybron 1964). Many attempts were also made to distinguish between surface and volume absorption potentials but it was found that, providing the radius and diffuseness parameters of the imaginary part are allowed to differ from those of the real part and the strength and form factors are optimized to fit the experimental data, both types of absorbing potential give practically equally good fits. Thus for practical purposes it does not matter which form is used, and to determine the form a more fundamental approach is required.

Many analyses of polarization data have shown that the optimum radius of the spin–orbit form factor is about 10 % less than that of the central term. This is a consequence of the shorter range of the nucleon–nucleon spin–orbit interaction compared with that of the central interaction.

Optical model analyses of elastic scattering and polarization data cannot give unique values of all the parameters of the potential; rather it is certain combinations that correspond to a particular set of data. Thus, for example, the fit to the data is

insensitive to variations of U and r_u (the radius parameter of the real part of the potential) that keep Ur_u^2 constant, and similarly for Wa_w. Since the calculations of the potential from nuclear matter considerations are insufficiently precise to resolve these ambiguities, it is usual to fix the parameters of the form factors to average values and then to adjust the potential depths, U, W and U_S to fit the data. It is then possible to compare on the same basis the variation of these potentials with energy and from nucleus to nucleus.

Many such analyses of nucleon scattering have now been made and it is found that the potentials are quite similar for all nuclei and vary rather slowly with the incident energy. The optical model is thus a successful way of describing elastic scattering in a wide range of conditions, and this provides confirmation of the overall correctness of the derivations of the potential from more fundamental considerations.

The most extensive analysis of neutron elastic scattering was made by Perey and Buck (1962) who fitted the differential cross sections, polarizations, total and reaction cross sections and strength functions for a wide range of nuclei from 4 to 25 MeV with a nonlocal potential of the form

$$V(\boldsymbol{r},\boldsymbol{r}') = V\{\tfrac{1}{2}(\boldsymbol{r}+\boldsymbol{r}')\}\frac{1}{(\pi\beta^2)^{3/2}}\exp\left\{-\left(\frac{\boldsymbol{r}-\boldsymbol{r}'}{\beta}\right)^2\right\} \tag{6.2}$$

where β is the range of the nonlocality. The equivalent local potential has been calculated by Wilmore and Hodgson (1964) and is consistent with most existing data on neutron scattering, except from very deformed nuclei.

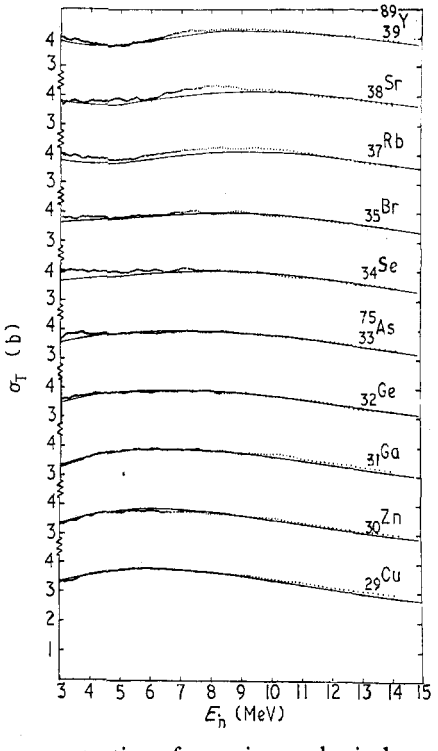

Figure 13. Total neutron cross sections for various spherical or vibrational nuclei compared with optical model calculations using the nonlocal potential of Perey and Buck. From Glasgow and Foster (1971).

A remarkable confirmation of the Perey–Buck potential is provided by the very extensive and accurate measurements of neutron and total cross sections made by Glasgow and Foster (1971). The cross sections calculated from the potential of Perey and Buck differ by less than 3% from the experimental values for 46 spherical or soft nuclei for neutrons from 3 to 15 MeV. The fit is considerably poorer, but still within about 20% for 19 hard deformed nuclei. Some of these results are shown in figures 13 and 14. This influence of the nuclear deformation

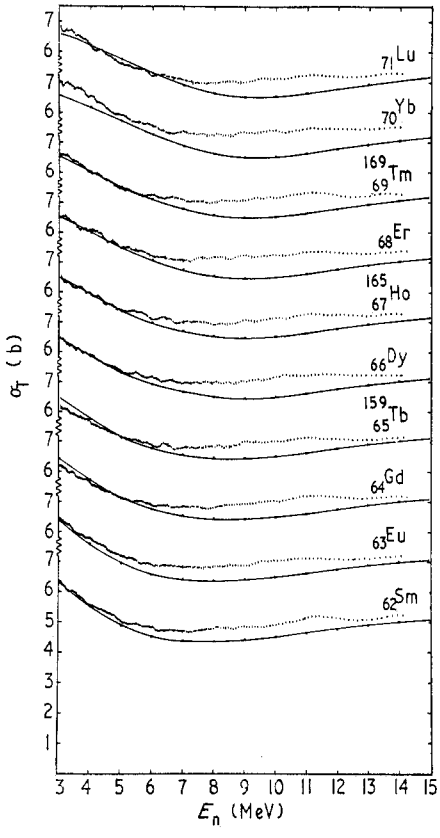

Figure 14. Total neutron cross sections for various hard deformed nuclei compared with optical model calculations using the nonlocal potential of Perey and Buck. From Glasgow and Foster (1971).

on the cross sections is to be expected and it is not surprising that it is not given by a spherical optical potential. It is possible to include this effect within the framework of the optical model by taking into account the coupling between the elastic and inelastic channels. For spherical nuclei this coupling is weak and so the elastic scattering is unaffected by the differences in energy level structure from one nucleus to the next, but for deformed or deformable nuclei the coupling may be so strong that this is no longer the case. These calculations are discussed in § 10.

The measurements of proton elastic scattering can be made to much higher accuracy, and this permits more detailed studies of the optical potential. Very many investigations have now been made, and have yielded expressions for the potential that can be used to calculate the cross sections with some confidence for many nuclei

over a wide energy range. Examples of the precision of optical model fits to differential cross sections and polarizations are shown in figures 15 and 16.

The real central potential has received the most detailed study, and it has been found to decrease linearly as the energy increases, with $dU/dE \simeq -0{\cdot}2$. For proton scattering this gives an extra term in the potential (Lane 1957) since the Coulomb potential decreases the energy of the proton in the nuclear interior. The magnitude of this term may be found by averaging the Coulomb field over the nuclear interior and multiplying by dU/dE; this gives $0{\cdot}4Z/A^{1/3}$ for $r_0 = 1{\cdot}25$ fm.

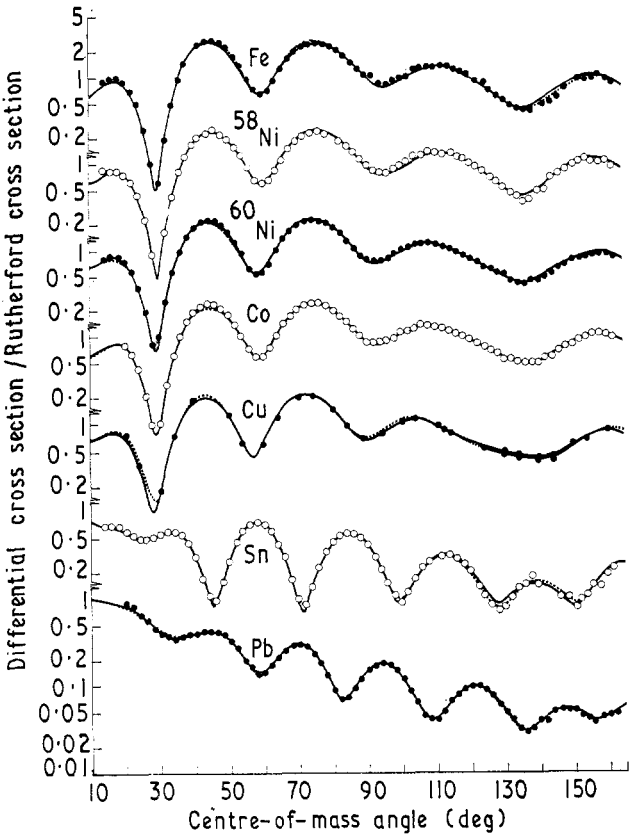

Figure 15. Differential cross sections for the elastic scattering of 30·3 MeV protons by a range of nuclei compared with optical model calculations with: full lines, a constrained spin–orbit potential; broken lines, an independent spin–orbit potential. From Satchler (1967).

An extensive analysis of the differential cross sections for the elastic scattering of 9–22 MeV protons by a range of nuclei (Perey 1963) showed that if the form factors are fixed to the average values $r_u = 1{\cdot}25$ fm and $a_u = 0{\cdot}65$ fm the depth of the real part of the potential is given in MeV by

$$V = 53{\cdot}3 - 0{\cdot}55E - 27(N-Z)/A + 0{\cdot}4Z/A^{1/3}. \qquad (6.3)$$

This shows the linear dependence on the energy and on the symmetry parameter $\alpha = (N-Z)/A$. This coefficient of the energy dependence is rather high, and values between 0·2 and 0·3 are found in more recent analyses.

The dependence of the optical potential on the symmetry parameter has also been found in studies of nuclear binding energies and Lane (1962) suggested that these results can be correlated by postulating a symmetry or isospin term in the nucleon–nucleus potential of the form

$$V_1(r) = \frac{4V_1}{A}\, \boldsymbol{t}.\boldsymbol{T} f(r) \tag{6.4}$$

where $\boldsymbol{t}$ and $\boldsymbol{T}$ are the isospin vectors of the incident particle and target nucleus respectively. This gives a term αV_1 in the proton potential and also a similar term $-\alpha V_1$ in the neutron potential, though the neutron scattering data are insufficiently accurate to show its presence. This isospin potential is also responsible for (p, n)

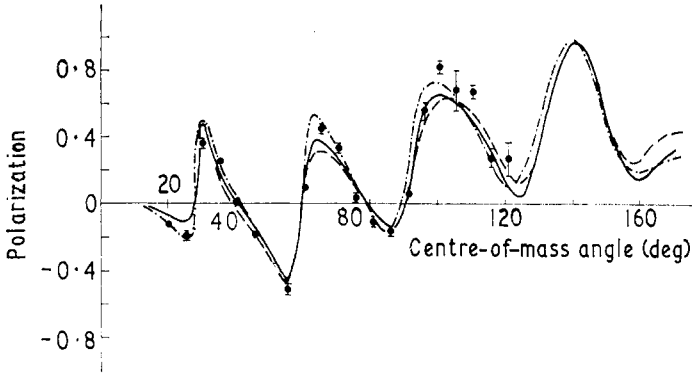

Figure 16. Polarization of 30 MeV protons elastically scattered by ^{60}Ni compared with optical model calculations with different forms of absorbing potential: full line, surface and volume absorption; broken line, surface absorption; chain line, volume absorption. From Greenlees and Pyle (1966).

reactions to the isobaric analogue state of the target nucleus, and the phenomenological analysis of the differential cross sections has enabled the form factor and strength of this term to be determined. The results are consistent with those obtained from proton elastic scattering.

Some accurate results of Perey *et al* (1968) have however thrown doubt on the method of obtaining the isospin potential from proton elastic scattering. They analysed the elastic scattering and polarization of 11 MeV protons for a range of nuclei with $50 \leqslant A \leqslant 70$, and found that when the real parts of the resulting optical potentials are plotted as a function of the symmetry parameter the points corresponding to the different nuclei fall on a series of curves, each characterized by a single value of the isospin T (see figure 17). A clue to the explanation of this result is provided by the observation of Greenlees *et al* (1968) that the integral of the real part optical potential per nucleon is constant to within a few per cent. Using a Saxon–Woods form factor this gives for the real potential depth

$$V = V_0 \Big/ \left(1 + \frac{\pi^2 a^2}{R^2}\right). \tag{6.5}$$

This may be converted to a relation giving V as a function of α and T by using the expressions $2T = \alpha A$ and $R = r_0 A^{1/3}$, so that

$$V = V_0 \Big/ \left\{1 + \frac{\pi^2 a^2}{r_0^2}\left(\frac{\alpha}{2T}\right)^{2/3}\right\}. \tag{6.6}$$

This relation is in qualitative accord with the results of figure 17 and it is remarkable that the expression is purely geometrical, with no reference to isospin. However, an isospin term must be present to account for (p, n) reactions to the isobaric analogue state, so this must be added to (6.5), together with the term $0{\cdot}4Z/A^{1/3}$ already mentioned. Thus

$$V = V_0 \Big/ \left(1+\frac{\pi^2 a^2}{R^2}\right) + U_1 \alpha + 0{\cdot}4Z/A^{1/3}. \tag{6.7}$$

This expression with the single adjustable parameter V_0 is in fair accord with the data of Perey *et al* (1968), as shown in figure 17, and a further phenomenological

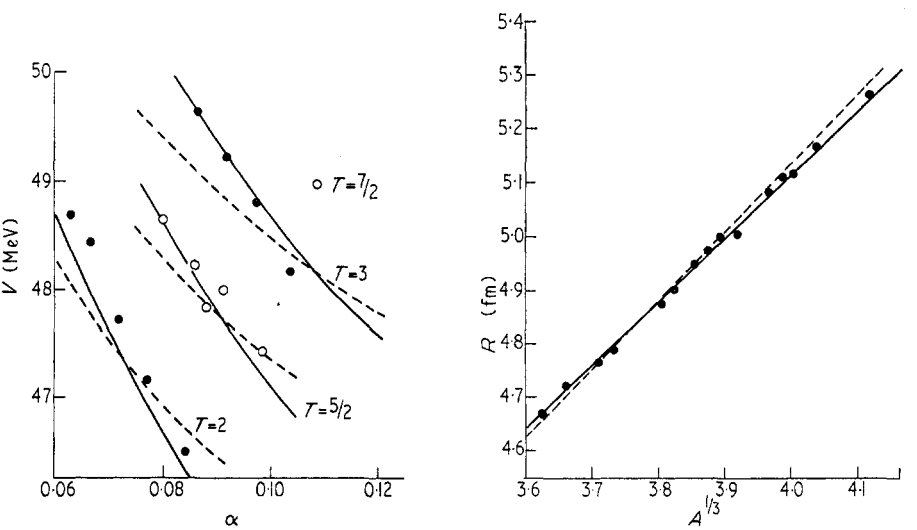

Figure 17. (*a*) Proton optical potentials, as a function of the nuclear symmetry parameter $\alpha = (N-Z)/A$, calculated from the expression for the real potential depth

$$V = \frac{106{\cdot}75A}{R^3(1+\pi^2 a^2/R^2)} + 24\alpha + \frac{0{\cdot}517T(1-\alpha)}{\alpha R}$$

compared with the experimental data of Perey and Perey (1968). (*b*) Comparison of the relationship between R and A with the data of Perey and Perey. In each case the broken line refers to a value $R = 1{\cdot}285A^{1/3}$ and the full line to $R = 1{\cdot}204A^{1/3} + 0{\cdot}305$. From Hodgson (1970).

adjustment gives quantitatively acceptable curves. Equation (6.7) enables the real part of the optical potential for protons to be calculated quite accurately for 11 MeV protons on nuclei with $50 \leqslant A \leqslant 70$, and a similar though more complicated expression may be obtained for other nuclei.

Examination of (6.7) shows that the original method of determining the strength of the isospin potential from proton elastic scattering is valid only for isobaric sequences, for which the A dependence of the first term is negligible. In other cases the method is not applicable unless the A dependence is accurately known in some other way and taken into account in the calculations.

In all this work on the isospin term it is assumed that its form factor is the same as that of the remainder of the real potential, but this is not unduly restrictive since the addition of a small surface-peaked potential to a volume potential of the same

radius has the effect of increasing the radius, and thus is equivalent to increasing the depth. It is however possible (Sinha and Edwards 1970) that the isospin potential has a smaller radius than the rest of the real potential, in which case the above result will not hold. It is in any case likely from nuclear matter calculation that the isospin term does not have the same form for all nuclei, but tends to be surface-peaked for light nuclei and of the volume form for heavy nuclei. It is thus desirable to use a calculated form factor for the isospin potential and to determine its strength by comparison with the (p, n) data.

There has been some work on the imaginary part of the isospin potential, but lack of knowledge of its form factor prevents any definite conclusions being drawn (Satchler 1967, Hodgson 1967). If it is assumed to be surface-peaked then a marked dependence on the symmetry parameter is found from analyses of proton elastic scattering. In order to separate the isospin dependence from that of purely geometrical origin it is necessary to make the corresponding analyses for neutrons, but these are at present insufficiently accurate to permit reliable conclusions. A more direct way of investigating the isospin dependence of the imaginary potential is from measurements of the S wave neutron strength function, and preliminary results of Newstead *et al* (1971) indicate values consistent with the observed symmetry dependence being largely of isospin origin.

The usual formulation of the optical model makes no reference to the spin of the target nucleus, but it is at least conceivable that this affects the scattering of nucleons and other nuclei. This possibility may be investigated by postulating a nuclear spin dependent term, calculating its observable consequences and seeing if they are found experimentally. There are many forms of spin dependent potentials that satisfy the general invariance requirements and can be constructed from the vectors $\boldsymbol{r}$, $\boldsymbol{p}$, $\boldsymbol{\sigma}$, $\boldsymbol{L}$ and $\boldsymbol{I}$ (the nuclear spin). In addition to the spin–orbit term, there are the nuclear spin dependent terms $\boldsymbol{I}.\boldsymbol{\sigma}$, $(\boldsymbol{I}.\boldsymbol{r})(\boldsymbol{\sigma}.\boldsymbol{r})$, $(\boldsymbol{L}.\boldsymbol{I})$, $(\boldsymbol{I}.\boldsymbol{\sigma})(\boldsymbol{L}.\boldsymbol{I})$ and $(\boldsymbol{\sigma}.\boldsymbol{p})(\boldsymbol{I}.\boldsymbol{p})$. Attention has so far been concentrated on the first and simplest of these, which is written in the form

$$V_{\mathrm{SS}}(r) = V_{\mathrm{SS}} f_{\mathrm{SS}}(r) \frac{\boldsymbol{I}.\boldsymbol{\sigma}}{I} \tag{6.8}$$

usually with a Saxon–Woods form factor $f_{\mathrm{SS}}(r)$. If the form factor parameters are chosen to be the same as the real central potential the spin–spin term may conveniently be included in the expression for the real potential depth, and as there are at present insufficient data to determine the form factor this is usually done.

It has not proved easy to find any evidence for the presence of this term. The polarization is directly dependent on the spin–orbit term and so analyses of polarization data, together with differential cross sections, enables its characteristics to be determined. The polarization might also be expected to be sensitive to the spin–spin term (6.8) but the measured polarizations of protons elastically scattered from nuclei with very different spin but otherwise similar characteristics show almost identical polarizations, while calculations indicate that the spin–spin term has no first-order effect on the polarization. Thus, at best, the differential cross sections and polarizations show only a second-order dependence on the spin–spin term, and so cannot be used to obtain a reliable indication of its presence.

The scattering phenomena directly sensitive to the target spin require polarized or at least aligned target nuclei, and such experiments are technically very difficult. Nevertheless several attempts to perform them have been made. The techniques

of nuclear alignment require a fairly thick sample, complicated surrounding apparatus and a high nuclear spin, so most investigations have used neutrons of about 1 MeV scattered by ^{59}Co and ^{165}Ho. No evidence for the presence of a spin–spin term has yet been obtained, though it is possible to set an upper limit to the value of the spin–spin potential V_{SS}. Thus, for example, the work of Nagamine *et al* (1970) on the total cross section of 1 MeV polarized neutrons on polarized ^{59}Co showed that $|V_{SS}| < 1{\cdot}0$ MeV.

Some measurements have been made by Batty and Tschalär (1970) of the depolarization parameter D, which is a measure of the change in polarization occurring in elastic scattering. Their results for 50 MeV protons elastically scattered by a range of nuclei gave no indication of the presence of a spin–spin term in the optical potential.

The introduction of the spin–spin term into the Schrödinger equation splits the single-particle states of orbital angular momentum L into components with total angular momenta $J = |L-S|$ to $(L+S)$, for $L \geqslant S$, where $\boldsymbol{S} = \boldsymbol{I}+\frac{1}{2}$ is the channel spin. The corresponding phase shifts thus pass through resonances at the appropriate energies, but in the normal scattering situation, when many reaction channels are open, the absorbing potential so broadens these states that they cannot be identified. At low energies in light nuclei, however, most if not all these reaction channels are closed, so the resonances are quite sharp, and this may provide one of the most favourable circumstances for the investigation of the spin–spin term.

A suitable case is the elastic scattering of protons and neutrons of a few MeV by ^{12}C. The cross sections are well known experimentally and so few phase shifts contribute that they can be obtained from the experimental data as a function of incident energy. Some of the resonances are due to single-particle states in the

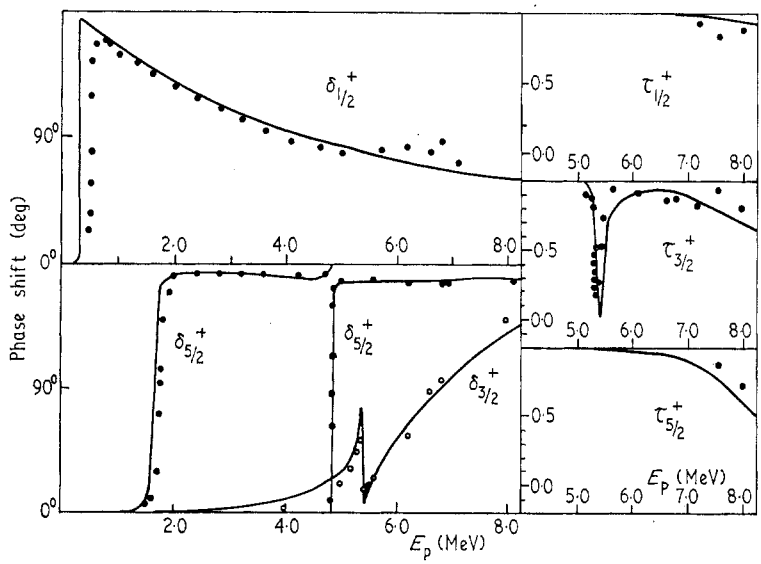

Figure 18. Comparison between the experimental phase shifts for the elastic scattering of protons by ^{12}C and coupled calculations using a rotational model with $\beta = -0{\cdot}5$ and a spin–spin term with $V_{ss} = 0{\cdot}37$ MeV. The quantity δ_{J^π} is the real part of the phase shift for the J^π partial wave, and $\tau_{J^\pi} = \exp(-2\eta)$ where η is the imaginary part of the phase shift for the J^π partial wave. From Mikoshiba *et al* (1971).

continuum, while others result from coupling to collective states of the target nucleus. Such a situation may be treated theoretically by the coupled channels theory discussed in § 10, and a series of studies of increasing refinement have been made in order to obtain an accurate description of these resonances (Pascolini *et al* 1969).

One of the most recent of these, by Mikoshiba *et al* (1971), obtained a very good overall fit to the data using a rotational collective model for ^{12}C, with deformation parameter $\beta = -0{\cdot}5$. It was also necessary to include a spin–spin term in the optical potential, with $V_{SS} \approx 0{\cdot}4$ MeV, consistent with previous estimates. This term is present when the target nucleus is virtually excited to the first 2^+ state. Some of their results for proton and neutron scattering are shown in figures 18 and 19. They also included a term in the potential proportional to L^2 which enables the state dependence of the potential to be taken into account. These calculations are complicated, and depend on many parameters, so it is not easy to be sure that the ambiguities have been thoroughly explored, but it does seem to be one of the most promising ways of investigating the spin–spin term.

There are some indications that the spin–spin term may significantly affect the strength functions; in particular it may be responsible for the systematic difference between the neutron S wave strength functions for odd and even nuclei around $A = 65$ (Rahman Kahn 1966). Additional evidence for the spin–spin term has been found from neutron S wave strength functions for isotopes of Nd, Sm and Ho by Newstead *et al* (1971). The magnitude of the spin–spin term may be calculated from the strength of the $\boldsymbol{\sigma}_i.\boldsymbol{\sigma}_j$ term in the nucleon–nucleon interaction, and this gives values around 0·1 MeV (Rahman Kahn 1966, Fisher *et al* 1966). A more recent calculation by Satchler (1971a) shows that substantially smaller values are obtained when core polarization is taken into account.

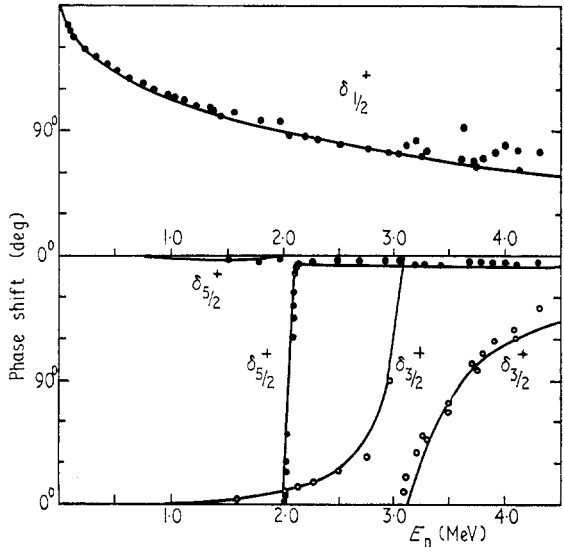

Figure 19. Comparison between the experimental phase shifts for the elastic scattering of neutrons by ^{12}C and coupled-channels calculations using the same model and parameters as the corresponding proton calculation shown in figure 18. From Mikoshiba *et al* (1971).

The next nuclear spin dependent potential in order of increasing complexity has a structure similar to the tensor force, and may be written

$$V_T(r) = V_T f_T(r)\{3(\boldsymbol{I}.\hat{\boldsymbol{r}})(\boldsymbol{\sigma}.\hat{\boldsymbol{r}}) - \boldsymbol{I}.\boldsymbol{\sigma}\}/2I. \tag{6.9}$$

The strength of this term may be found by comparing the total cross sections for polarized particles on polarized nuclei with the polarization axes parallel and anti-parallel and in the beam direction and perpendicular to it (Fisher 1971). Estimates of V_T from existing data give values consistent with zero and with the small values obtained by Satchler (1971a).

The electrostatic interaction between an incident charged particle and a nucleus may easily be taken into account by adding to the optical potential the electrostatic potential due to a uniformly charged sphere. In addition, there are other small electromagnetic effects for both charged and uncharged particles due to the interaction of the magnetic moment of the incident particle with the electrostatic field of the nucleus and these can be represented by a potential of the form

$$V_{MM}(r) = \frac{\mu - a}{2}\left(\frac{\hbar}{mc}\right)^2 \frac{1}{r}\frac{dV_C(r)}{dr}\boldsymbol{L}.\boldsymbol{\sigma} \tag{6.10}$$

where μ is the magnetic moment of the incident nucleon, $a = \frac{1}{2}$ for protons and $a = 0$ for neutrons, and $V_C(r)$ is the electrostatic Coulomb potential. Apart from the radial dependence, which falls off much more slowly ($\sim r^{-3}$) at large distances, this is very similar to the spin–orbit potential, so in most circumstances any effects due to magnetic moment scattering are absorbed by that term. In the case of scattering at very small angles, however, such a term may have appreciable effects both on the differential cross section and on the polarization. Since the differential cross section for the elastic scattering of protons rises so rapidly towards small angles it is more convenient to investigate these magnetic moment effects in the differential cross section for neutron scattering and in the polarization for proton scattering. Several studies have shown that the magnetic moment effects are indeed observed, and that their magnitude is in accord with the theoretical calculations (Monahan and Elwyn 1964).

The incident nucleon may also be polarized by the Coulomb field of the target, and the induced electric dipole moment can interact with the Coulomb field, giving an additional potential

$$V_{DM}(r) = -\alpha E^2/2 \tag{6.11}$$

where α is the electric polarizability and E the electric field. This potential is significant only outside the nucleus, where it becomes

$$V_{DM}(r) = -\alpha Z^2 e^2/2r^4. \tag{6.12}$$

In principle it should be possible to compare the results of calculations including this potential with experimental data on the elastic scattering of neutrons, and hence to determine the electric polarizability of the neutron. In practice, however, the effects are so small that they can readily be absorbed by small changes in the real part of the optical potential.

7. The elastic scattering of deuterons

Deuterons have several special features that complicate the way they are scattered by nuclei. They are very loosely bound, and are therefore easily broken up when they encounter the nuclear field. The scattering is thus rather sensitive to

the nuclear structure and it is correspondingly more difficult to define overall optical potentials. The charge and mass centres of the deuteron are significantly separated, and this gives rise to forces tending to twist and break the deuteron even before it encounters the nuclear field. Finally the deuteron has spin one so that the polarization phenomena accompanying the scattering are much more complicated than for nucleons; to specify the polarization it is necessary to define not only the vector polarization as for particles of spin $\frac{1}{2}$, but also three tensor polarizations as well.

The possibility that the deuteron can be broken up by the Coulomb field alone must be carefully considered since it could take place well beyond the region where the optical potential is appreciable, and thus could not be represented by it. Calculations of the Coulomb breakup process have, however, shown that it is negligible except in the region of the nuclear field, and so it can be taken into account by the optical potential.

Discrete ambiguities are encountered in the optical model analysis of the scattering of deuterons and heavier particles. It is found that several potentials of depths around 50, 100, 150, ... MeV all give equally good fits. This may be understood quantum mechanically if one partial wave is considered. If the potential is progressively deepened, more and more waves are drawn into the nuclear region, and if a good fit is obtained with one depth, an equally good fit is obtained when the potential is deepened sufficiently to bring in just one extra half wave, since the asymptotic wavefunction is then unaltered. This is exact for one partial wave, but it turns out that the different partial waves keep nearly in step in this respect, so it applies to the whole angular distribution as well. Then there is phenomenologically a whole series of potentials giving very similar fits.

This ambiguity may be resolved by calculating the deuteron potential from the constituent neutron and proton potentials. Although it is subject to many uncertainties, the calculation is sufficiently accurate for this purpose. The simplest expression for the deuteron optical potential is just the sum of the constituent nucleon potentials evaluated at half the deuteron energy. A more accurate expression may be obtained by averaging this over the internal wavefunction $\phi_D(\boldsymbol{x})$ of the deuteron so that (Watanabe 1958)

$$V_D(r) = \int \phi_D^2(\boldsymbol{x}) \{V_n(\boldsymbol{r}+\boldsymbol{x}/2) + V_p(\boldsymbol{r}-\boldsymbol{x}/2)\} \, d\boldsymbol{x} \tag{7.1}$$

where $\boldsymbol{x} = \boldsymbol{r}_n - \boldsymbol{r}_p$ is the separation between the neutron and proton in the deuteron, and $V_n(\boldsymbol{r}+\boldsymbol{x}/2)$ and $V_p(\boldsymbol{r}-\boldsymbol{x}/2)$ are the neutron and proton optical potentials, usually evaluated at half the deuteron energy. Calculations with this expression show that the correct deuteron potential has a depth of rather less than the sum of the constituent neutron and proton depths (ie about 100 MeV) and this value is used in all optical model analyses of deuteron elastic scattering.

Many optical model analyses of deuteron elastic scattering have now been made, and it has been found possible in most cases to obtain a good fit to the differential cross sections. The optimum form factors have a radius for the imaginary part greater than that of the real part. Some investigations have covered a range of nuclei at different energies, and formulae have been obtained expressing the potential as a function of the appropriate variables. Thus for example Perey and Perey (1963) analysed an extensive set of data and obtained the expression for the real part of the potential

$$U = 81 + 2{\cdot}0Z/A^{1/3} - 0{\cdot}22E \tag{7.2}$$

where energies are in MeV, with form factor parameters $r_u = 1{\cdot}15$ fm, $a_u = 0{\cdot}81$ fm, $r_w = 1{\cdot}34$ fm and $a_w = 0{\cdot}68$ fm.

Such expressions are not as accurate as for nucleon scattering due to the greater sensitivity of deuteron scattering to the surface potential and hence to details of nuclear structure. Unfortunately it has not yet been found possible to turn this sensitivity to good account and use it to determine specific features of the nuclear surface region.

The polarization phenomena associated with the elastic scattering of deuterons are much more complicated than those of nucleons, because the description of the state of polarization of a beam of particles of spin one requires not only a vector polarization as for nucleons, but three independent tensor polarizations as well. There are also several possible spin dependent interactions that could be included in the deuteron optical potential, and an examination of the forms that can be constructed from the vectors $\boldsymbol{r}$, $\boldsymbol{L}$, $\boldsymbol{p}$ and $\boldsymbol{S}$, subject to general invariance and symmetry restrictions, gives the forms (Satchler 1960)

Spin–orbit $$V_S(r) = U_S h_s(r) \boldsymbol{L}.\boldsymbol{S} \tag{7.3}$$

Tensor 1 $$V_{T1}(r) = U_{T1}\{(\boldsymbol{S}.\boldsymbol{r})^2/r^2 - \tfrac{2}{3}\} f_{T1}(r) \tag{7.4}$$

Tensor 2 $$V_{T2}(r) = U_{T2}\{(\boldsymbol{S}.\boldsymbol{p})^2 - \tfrac{2}{3}\boldsymbol{p}^2\} f_{T2}(r) \tag{7.5}$$

Tensor 3 $$V_{T3}(r) = U_{T3}\{(\boldsymbol{L}.\boldsymbol{S})^2 + \tfrac{1}{2}(\boldsymbol{L}.\boldsymbol{S}) - \tfrac{2}{3}\boldsymbol{L}^2\} f_{T3}(r) \tag{7.6}$$

where the form factors are functions of r that are not yet determined. Using any of these forms for the deuteron spin dependent potential, the polarization produced in an unpolarized beam can be calculated, or alternatively the change in polarization of a beam already polarized.

It is in principle possible to investigate the presence of these forces, and to determine their magnitudes, by comparing the results of optical model calculations with the appropriate measurements. In practice, however, it is difficult to determine the polarization of a deuteron beam. It is somewhat easier, though still difficult, to produce a deuteron beam of known polarization, and then to measure the asymmetry of the elastically scattered deuterons, and some measurements have been made in this way.

Some of the earliest investigations of the deuteron spin dependent potential were made with 21·6 MeV deuterons on ^{40}Ca, and the results were analysed by Raynal (1963). He found that it is possible to obtain a good overall fit to the differential cross section and to the vector and tensor polarizations with a spin–orbit potential alone; there was no need to include a tensor potential. This is in accord with calculations of the magnitude of the tensor potential, which indicate that it is very small (Testoni and Gomes 1966).

The deuteron polarization has also been measured by Kossanyi-Demay and Mayer (1967) and their results for 21·6 MeV deuterons on ^{58}Ni and ^{60}Ni are shown in figure 20. An extensive analysis by Schwandt and Haeberli (1969) of the differential cross section and vector and tensor polarizations of 5 to 34 MeV deuterons by ^{40}Ca gave the following expressions for the deuteron potential

$$\left.\begin{array}{lll} U = 115 - 0{\cdot}3E, & r_u = 1{\cdot}05, & a_u = 0{\cdot}85 \\ W_s = 12{\cdot}3 - 0{\cdot}01E, & r_w = 1{\cdot}71 - 0{\cdot}01E, & a_w = 0{\cdot}48 + 0{\cdot}007E \\ U_s = 6{\cdot}5, & r_s = 0{\cdot}9, & a_s = 0{\cdot}6 \end{array}\right\} \tag{7.7}$$

where energies are in MeV and distances in fermis. Further discussion of deuteron elastic scattering together with a table of potentials obtained up to 1966 may be found in the review by Hodgson (1966).

Many detailed attempts have been made to calculate the deuteron optical potential from the constituent neutron and proton potentials (Testoni and Gomes 1966, Mukherjee 1968, Rihan and Sharaf 1969, Satpathy *et al* 1969, Bencze and Doleschall 1970, Samaddar *et al* 1970, Keaton 1971). The overall features can be obtained from the simple folding expression (7.1) but to improve on this requires much detailed formalism unsuitable for summary here.

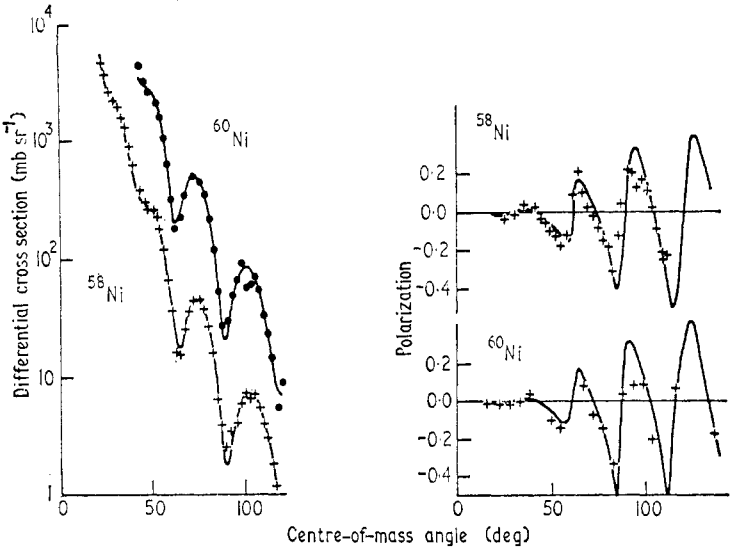

Figure 20. Differential cross section and vector polarization of 21·6 MeV deuterons elastically scattered by ^{58}Ni and ^{60}Ni, compared with optical model calculations with inclusion of a spin–orbit potential. From Kossanyi-Demay and Meyer (1967).

There is, however, one feature of this work that deserves to be mentioned because of its bearing on the nucleon optical potentials. These are known on theoretical grounds to be partly local and partly nonlocal, but as they are phenomenologically equivalent for elastic scattering analyses they are usually for convenience taken to be wholly local. There are, however, two ways of calculating the deuteron potential, even if this is taken to be wholly local as well. Thus either one can start from local nucleon potentials and hence obtain the local deuteron potential or one can start with the equivalent nonlocal nucleon potentials, calculate the corresponding nonlocal deuteron potential and then find its local equivalent. This has been done by Samaddar and Mukherjee (1971) and they find that these deuteron potentials have different energy dependences. It is thus possible in principle, by comparison with the phenomenological deuteron potentials, to find the extent to which the nucleon potentials are nonlocal, and the extent of their intrinsic energy dependence.

The calculation of the deuteron optical potential is made more difficult by the ease with which the deuteron may be broken up in the nuclear field. The effect of this process has been studied by Johnson and Soper (1970) using an adiabatic

approximation, and they obtained a set of coupled equations for the elastic scattering and deuteron breakup wavefunctions. Solution of these equations shows that they account very well for the partial waves corresponding classically to reactions in the region of the nuclear surface, and this improves the agreement with the experimental data.

8. The elastic scattering of helions and tritons

Helions and tritons are more strongly bound than deuterons and so Coulomb breakup effects are negligible, and as they have spin $\frac{1}{2}$ the polarization phenomena are similar to those of nucleons. They interact strongly with the nuclear field and so their scattering is rather sensitive to the potential in the surface region, making it more difficult to find overall optical potentials.

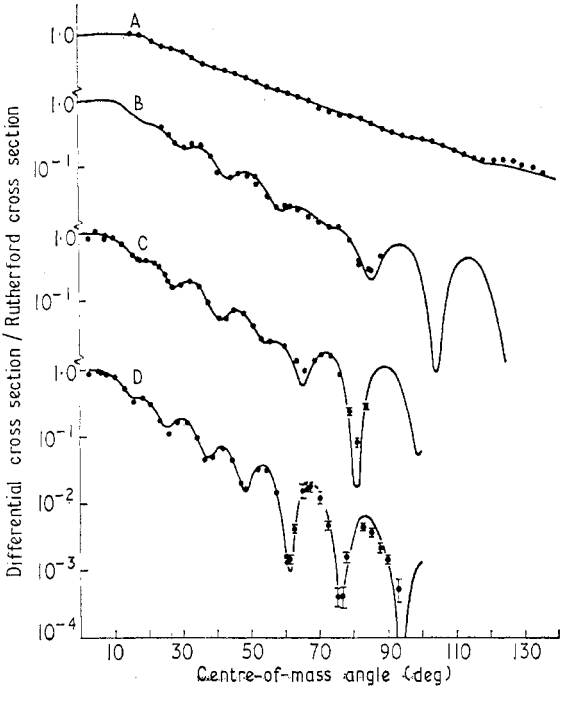

Figure 21. Differential cross sections for the elastic scattering of helions by ^{58}Ni compared with optical model calculations. A, E = 22 MeV (Los Alamos); B, E = 33 MeV (Argonne); C, E = 37·7 MeV (Gibson *et al*); D, E = 43·7 MeV (Gibson *et al*). From Gibson *et al* (1967).

The mass of the helion and triton ensures that at energies high enough for the effects of the nuclear field to be appreciable a substantial number of partial waves contribute to the interaction. It is then possible to describe many of the features of the elastic scattering and polarizations by diffraction models, or by parametrizing the elements of the scattering matrix by continuous functions of the orbital angular momentum quantum number (Springer and Harvey 1965, Fernandez and Blair 1970).

Many optical model analyses have also been made, and a typical study of the energy variation of the differential cross section is shown in figure 21. The potential depth ambiguity is particularly troublesome for helions and tritons because it is

often found that there are many discrete potentials giving practically identical fits, and the calculations of the potential from the component nucleon–nucleus potential are not sufficiently accurate to show which must be chosen, as was the case for deuteron scattering. They do, however, indicate a value of the real potential around 150 MeV, so depths similar to this are most often used.

For a particular nucleus it is usually possible to find empirical formulae to represent the energy variation of the real and imaginary potentials when fixed form factors are used. An analysis of 20 MeV helion scattering by a range of nuclei gave potentials with a linear dependence on A (Gibson *et al* 1967). A particularly extensive analysis of helion and triton scattering has been made by Becchetti and Greenlees (1969) who find that it is quite well fitted by the potentials

Helion
$$\left.\begin{aligned} U &= 136{\cdot}4 - 0{\cdot}17E + 55(N-Z)/A \\ W_v &= 41{\cdot}3 - 0{\cdot}33E + 63(N-Z)/A \end{aligned}\right\} \quad (8.1)$$

Triton
$$\left.\begin{aligned} U &= 165 - 0{\cdot}17E - 110(N-Z)/A \\ W_v &= 46{\cdot}0 - 0{\cdot}33E - 110(N-Z)/A \end{aligned}\right\} \quad (8.2)$$

with the form factor parameters $r_u = 1{\cdot}2$, $a_u = 0{\cdot}72$, $r_w = 1{\cdot}4$, $a_w = 0{\cdot}86$ (energies are in MeV and distances in fermis). These parameters are not unique, and many other sets give comparable fits. Inclusion of a spin–orbit potential slightly improves the fit, but in the absence of extensive polarization data it was not used in the analysis.

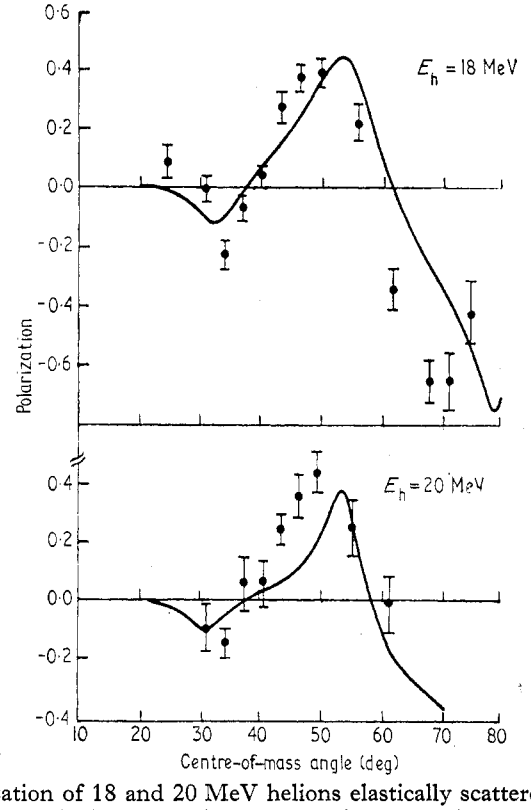

Figure 22. Polarization of 18 and 20 MeV helions elastically scattered by ^{12}C compared with optical model calculations with a spin–orbit potential $V_s = 4, 4{\cdot}5$, $r_s = 1{\cdot}0$, $a_s = 0{\cdot}5$. From McEver *et al* (1970).

Rather few measurements of the polarization of elastically scattered helions and tritons have been made. A recent example of such a measurement is shown in figure 22 together with optical model curves. Theoretical considerations indicate that the helion and triton spin–orbit potentials should be similar in form to the corresponding nucleon potential, with a strength three times smaller, and this is consistent with the available measurements.

The helion and triton optical potentials may be combined to give a general mass-three potential, just as the neutron and proton potentials can be combined in the nucleon potential. If the same form factors are used, the difference between the helion and triton potential depths indicates the presence of an isospin term similar to the corresponding term in the nucleon potential. The potentials also show a dependence on the symmetry parameter due to nuclear structure effects, and this may be determined by analysis of measurements on isotopic or isobaric sequences. In one of these investigations, comparison between the helion and triton optical potentials at 21 MeV shows that the imaginary part of the potential depends on the nuclear symmetry parameter, and that most of this is not of isospin origin (Urone *et al* 1971). The energy was not high enough to permit investigation of the real part of the isospin potential.

Further discussion of helion and triton elastic scattering together with a table of the potentials obtained up to 1968 may be found in the review by Hodgson (1968).

9. The elastic scattering of α particles

The α particle is a tightly bound spinless structure, and this simplifies the description of how it is scattered by nuclei. Its charge and mass ensure that a substantial number of partial waves contribute when the energy is above the Coulomb barrier, so that the diffraction and parametrized scattering amplitude

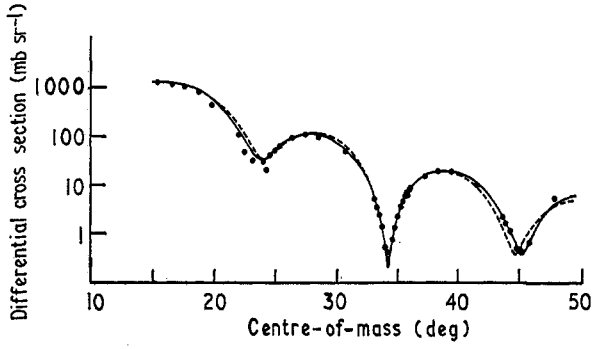

Figure 23. Differential cross sections for the elastic scattering of 42 MeV α particles by ^{44}Ca compared with: full line, optical model calculations with a four-parameter potential; broken line, the distribution given by the parameterization of the scattering amplitude. From Fernandez and Blair (1970).

models are very successful in many respects. This is shown by the comparison in figure 23 between the experimental data for the elastic scattering of 42 MeV α particles by calcium and the two types of theoretical description.

As for helions and tritons, the potential depth ambiguities constitute a serious difficulty. These have been extensively studied for α particle scattering and it is again found that several potentials give equally good fits within the range indicated

by calculations from the nucleon–nucleon potential. It is not possible to resolve these ambiguities by coupled channels calculations (Eberhard and Robson 1971). There have been many optical model analyses of α particle scattering with both four-parameter (U, W, r_0, a) and six-parameter (U, r_u, a_u, W, r_w, a_w) potentials. In many cases the adequate fit is obtained with a four-parameter potential, in which

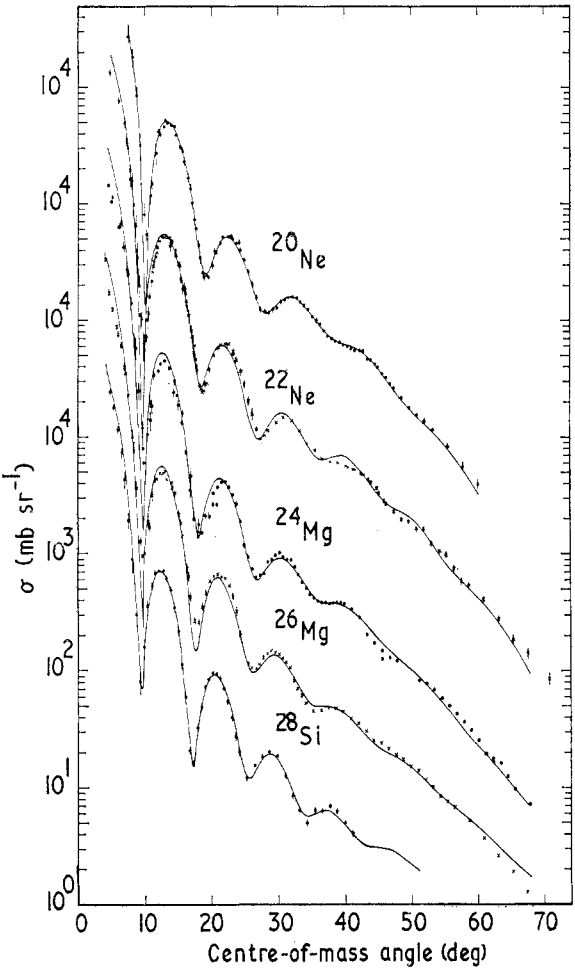

Figure 24. Elastic scattering of 104 MeV α particles by some light nuclei compared with optical model calculations. Note that the curves are vertically displaced from each other by a factor of 10. From Rebel (1971).

the form factors of the real and imaginary parts are the same, but if the data are extensive a significant improvement can usually be obtained with a six-parameter potential, and then it is found that the radius of the imaginary potential is optimally 20–30% greater than that of the real potential, typical values being $r_u = 1{\cdot}1$ fm, $r_w = 1{\cdot}4$ fm. An example of the precision that can now be attained is shown in figure 24.

The elastic scattering of α particles is particularly sensitive to the potential in the region of the nuclear surface, and may thus be used to study the radii of nuclei.

An indication of this sensitivity is shown by the cross sections for the elastic scattering of α particles by some calcium isotopes in the neighbourhood of a minimum (figure 25). The angle at which the minimum occurs can be measured to 0·1°, and hence a precise value of the nuclear radius can be found. If this is done for a series of isotopes, an accurate measure of the variation of the nuclear matter radius through the sequence is obtained, although the absolute value depends on the other parameters of the potential. Fernandez and Blair (1970) have used several different definitions of the nuclear radius, and find that they give very similar results for variations through isotopic sequences.

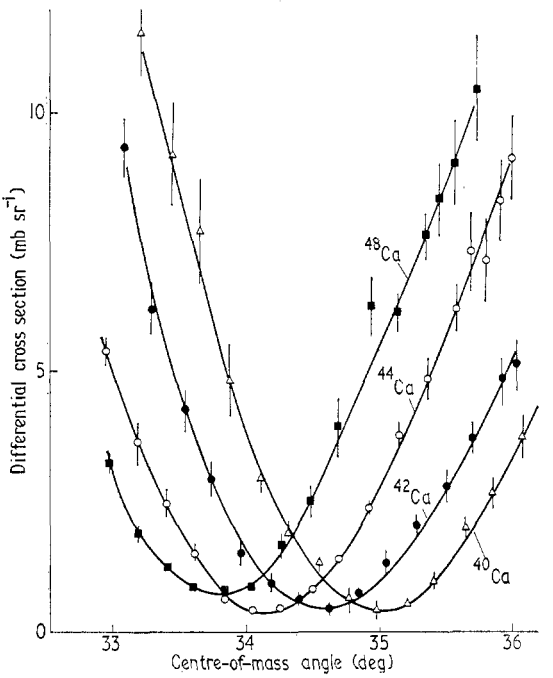

Figure 25. Differential cross sections for the elastic scattering of 42 MeV α particles by the Ca isotopes in the region of the minimum. From Fernandez and Blair (1970).

If these results for the nuclear matter radii are combined with the nuclear charge distributions obtained from electron elastic scattering then detailed information about the changes in neutron and proton density distributions from one nucleus to the next may be obtained. Some of this work has been reviewed by Jones (1970). The same surface sensitivity also makes it possible to determine the nuclear shape by analysing elastic and inelastic cross sections together by the coupled channels method. Some of this work is described in § 10.

Several attempts have been made to calculate the real part of the α particle potential from simpler interactions using folding procedures similar to those used for nucleons (see § 2). There are basically two ways of doing this: by a single folding from a nucleon–α potential or by a double folding from a nucleon–nucleon potential. The parameters of the nuclear matter distribution are treated as adjustable, and the real potential found in this way is supplemented by a phenomenological imaginary potential. The single folding procedure was used by Jackson and Kembhavi (1969) and by Morgan and Jackson (1969) using Gaussian and Yukawa

forms for the effective interaction, and optimization of the two parameters. The Gaussian interaction was found to give the better results as it is sufficiently peaked to give the required behaviour in the surface region. The fits to the experimental data obtained with this model are comparable in quality to those found with the standard optical model and require fewer adjustable parameters. A more detailed analysis has been made by Lilley (1971) using the phenomenological α–nucleon potentials fitted by Satchler *et al* (1968) to the p–α and n–α phase shifts, and he finds that the calculated potentials are consistent with those obtained by phenomenological analyses of the data.

The double folding procedure has been used by Budzanowski *et al* (1970) with an effective nucleon–nucleon interaction of the Gaussian, Yukawa and McManus forms, together with the matter distributions for the α particle and the target nucleus. The differential cross section for the elastic scattering of 27·5 MeV α particles by ^{59}Co calculated from these potentials gave only a qualitative fit to the data, being of the correct shape but too low in the forward direction. This is not unexpected, since resonating group calculations of the α–nucleon interaction have shown that it is not possible to obtain a satisfactory potential by simple folding of the free nucleon–nucleon interaction, due mainly to the neglect of antisymmetrization. It is thus preferable to use an effective α–nucleon interaction fitted directly to the data.

This and other work (Fernandez and Blair 1970) show that the elastic scattering of α particles is sensitive only to the potential in the surface region. Provided the real part of the potential is correct in this region it is immaterial what value it has in the nuclear interior, so that the volume integral of the potential is not a physically useful quantity (Weisser *et al* 1970), in contrast to the situation for nucleon scattering (see § 2). Physically this is because the α particles interact strongly in the region of the nuclear surface, while nucleons are more likely to penetrate to the nuclear interior. The α particle is thus a useful probe of the nuclear surface.

The elastic scattering of α particles shows several apparently anomalous features, some of which make an optical model analysis rather difficult, but which can give information on nuclear structure that cannot be obtained from the scattering of lighter particles.

The first of these features is the pronounced peak sometimes found in the extreme backward direction around 180°; this is sometimes called the 'glory effect' by analogy with a similar phenomenon in meteorology. It was at one time thought that this feature is not given by the optical model, but detailed calculations showed that it is indeed given automatically by the potentials fitted to the data at smaller angles. The width of the peak is in accord with that observed, but it is not possible to make a comparison of the magnitude because of the presence of the second anomaly described below. The glory effect is essentially due to the cumulative reinforcement of the contributions from several even partial waves with orbital angular momenta around that given by the classical input parameters. A typical cross section showing the glory effect is illustrated in figure 26.

The second anomaly is the rise in the cross section at backward angles that occurs for some nuclei but not for others. It is possible to fit the overall features of these distributions with the optical model by adjusting the parameters in each case, but they cannot all be fitted by the same potential. In the case of 22–29 MeV α particles, the effect is found to be strong for ^{36}A, ^{40}Ca and ^{39}K, weak for ^{42}Ca and ^{41}K, and absent for ^{40}A, ^{44}Ca and ^{48}Ca.

There were some attempts (Schmeing 1970) to explain this anomaly as a consequence of the α clustering that has been thought to occur in the surface region of nuclei (Wilkinson 1961) but a detailed calculation (Thompson 1971) showed that this hypothesis is untenable. A much more convincing explanation has been suggested by Eberhard (1970) who connects it with the level density in the residual nuclei in the open channels. It is a special characteristic of α particle interactions that they bring quite high angular momenta into the nucleus, and if final states of sufficiently high J are not available in the reaction channels the corresponding flux must be re-emitted into the elastic channel, thus raising the cross section in the backward direction. A detailed examination of the final state level densities showed that this effect is to be expected for just those nuclei where it is found to occur.

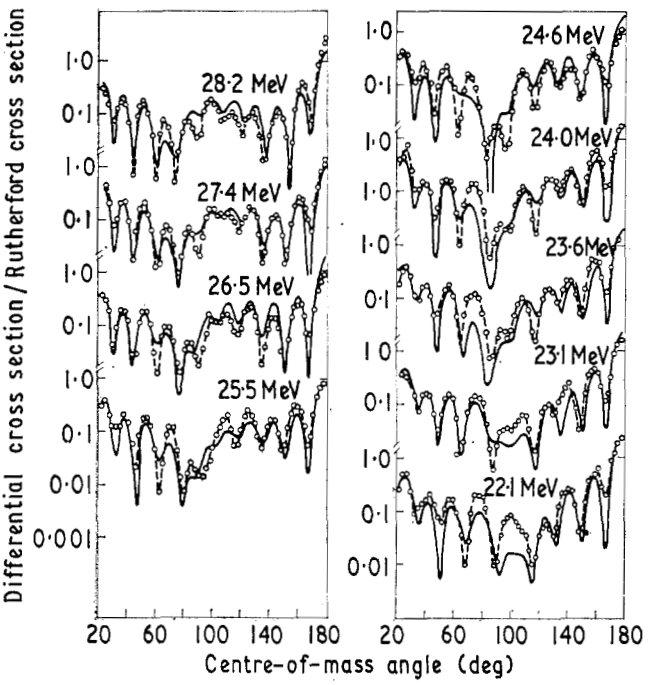

Figure 26. Differential cross sections for the elastic scattering of α particles at several energies from ^{39}K compared with optical model calculations: broken line, experimental curve; full line, optical model best fit. These show that the maximum in the cross section at 180° is very well given by the model. From Budzanowski *et al* (1968).

This effect may be brought within the optical model by allowing the imaginary potential to depend on the orbital angular momentum (Bisson *et al* 1970, Chatwin *et al* 1970); a suitable parametrization is

$$W_L(r) = W(r)/[1+\exp\{(L-L_c)/\Delta L\}] \tag{9.1}$$

where L_c is similar to the classical value for surface interactions. This expression ensures that for the higher partial waves the absorption potential is small, reflecting the physical fact that the scarcity of final states in the reaction channel prevents absorption taking place.

The third anomaly found in connection with the elastic scattering of α particles concerns the resonances that are sometimes observed in the excitation functions,

particularly at back angles. These resonances are due to states in the compound nucleus of high J and they are particularly prominent because, as just mentioned, they sometimes have difficulty in decaying into the reaction channels. This distinguishes the situation from the case of lighter particles where the compound nuclear resonances are very numerous and readily decay into nonelastic channels. Several cases of these compound nucleus resonances have been found in the elastic scattering of α particles, and a well marked example is the broad maximum in the backward scattering of α particles by ^{39}K and ^{40}Ca around 24 MeV which may be fitted by modifying the reflection coefficient for $L = 10$ (Budzanowski *et al* 1967).

10. Inelastic scattering

The optical model may be extended by taking into account explicitly not only the elastic channel but one or more nonelastic channels as well. The equations for the wavefunctions in these channels are coupled together, so this is particularly useful if the coupling between the channels is strong, as in the case, for example, of inelastic scattering with the excitation of collective states.

These equations may be obtained by expanding the total wavefunction in terms of the wavefunctions $\psi_\alpha(\boldsymbol{r})$ in the elastic and inelastic channels, and of the target nucleus in its ground and excited states $\phi_\alpha(\boldsymbol{\xi})$. Thus

$$\Psi(\boldsymbol{r}, \boldsymbol{\xi}) = \sum_\alpha \psi_\alpha(\boldsymbol{r})\,\phi_\alpha(\boldsymbol{\xi}) \tag{10.1}$$

where α labels the states of the target. Substituting this in the Schrödinger equation for the whole system and integrating out the angular dependence in the usual way gives a series of coupled radial differential equations for the wavefunctions in the elastic and inelastic channels (Buck 1963, Buck *et al* 1963, Tamura 1965). These may be solved using the optical potential for the interaction and the collective model wavefunctions for the nuclear states. If the macroscopic rotational or vibrational model is used, the only additional parameters are those representing the static or dynamic nuclear deformations.

This formalism makes it possible to analyse in a unified way the differential cross sections through a region of varying nuclear deformation. The cross sections depend on the deformation, but they may all be accounted for by appropriate values of the deformation parameter, the optical potential remaining unchanged. This has been done for 17 MeV protons elastically scattered by some heavy nuclei (Perey 1964). A formal investigation of the effects of nuclear deformation in the optical potential has recently been made by Mackintosh (1971).

To first order, the inelastic cross sections for the one-step excitations are proportional to the square of the corresponding deformation parameter and thus provide an accurate way of determining them. In his pioneer work, Buck (1963) applied the coupled-channels formalism to fit the elastic and first inelastic cross sections with excitation of the lowest 2^+ states of several medium weight nuclei, and the β_2 deformation parameters he obtained were in good accord with those obtained by other methods. Analysis of the elastic and inelastic scattering of composite particles provides an even better way of determining the shapes of nuclei because of the sensitivity of the interaction to the nuclear surface. Several such analyses have been made with α particles, and have enabled the higher order deformations to be determined. A recent example of such an analysis, showing the sensitivity of the

cross section to the β_4 deformation, is shown in figure 27. It is notable that the calculated cross sections for the excitation of the 4^+ state differ significantly for $\beta_4 = 0{\cdot}11$ and $\beta_4 = -0{\cdot}11$, so that the sign as well as the magnitude of β_4 can be obtained. The cross section is finite even for $\beta_4 = 0$ since the 4^+ state can be excited by a process proportional to $\beta_2{}^2$ that increases the spin by 2 acting twice, as well as by one proportional to β_4 that excites it directly.

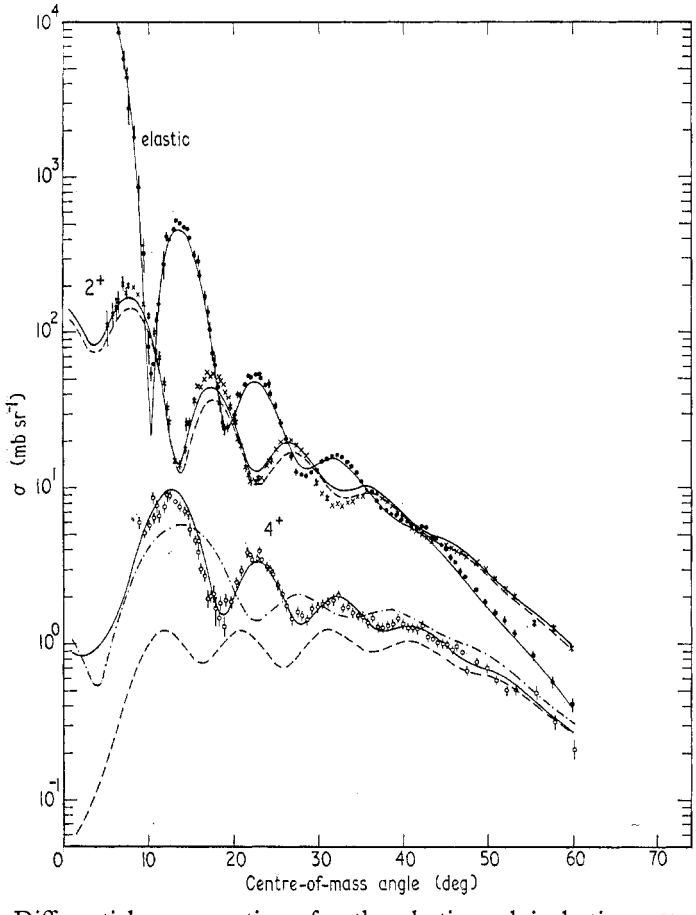

Figure 27. Differential cross sections for the elastic and inelastic scattering of 104 MeV α particles by ^{20}Ne compared with coupled-channel calculations showing the sensitivity to the β_4 deformation: full line, $\beta_2 = 0{\cdot}34$, $\beta_4 = 0{\cdot}11$; broken line, $\beta_2 = 0{\cdot}34$, $\beta_4 = 0{\cdot}0$; chain line, $\beta_2 = 0{\cdot}34$, $\beta_4 = -0{\cdot}11$. From Rebel (1971).

The coupled equations automatically give resonant cross sections at the energies of the collective excitations, just as the simple optical model gives them when the energy in the compound system corresponds to that of a single-particle state. In most cases, however, the resonances are so broadened by the imaginary part of the effective interaction that they are not observable. An important exception is the situation for some light nuclei at low energies, when most or all the nonelastic channels are closed. The most recent analysis of this type is that of Mikoshiba *et al* (1971) and as described in § 6 this has yielded information on the spin–spin term in the optical potential.

11. Compound nucleus reactions

It was shown in § 4 that many elastic scattering cross sections, particularly at low energies, have an appreciable compound nucleus component, and this must be calculated and subtracted before an optical model analysis can be made. In such cases the compound nucleus calculation is essential for the optical model analysis, and as it relies very largely on optical model penetrabilities it is appropriate to describe it here.

The theory of compound nucleus reactions was initially developed by Hauser and Feshbach (1952) and has since then been refined by many authors, notably by Moldauer (1961, 1964a, b). The full formalism of this theory is quite complicated, and involves substantial angular momentum algebra, so only the physical ideas will be described here.

The essential idea is very simple: a certain amount of flux representing the incident beam enters the target nucleus to form the compound nucleus, and it subsequently escapes through the open reaction channels. It is possible to define for each of these channels a transmission coefficient T_α that represents the readiness of the channel to transmit flux; in terms of the scattering matrix element

$$T_\alpha = (1 - |S_{\alpha\alpha}|^2). \tag{11.1}$$

It is then evident that the cross section for the reaction from the channel α to the channel β is proportional to the product of the corresponding transmission coefficients, divided by the sum of the transmission coefficients in all the channels, and a detailed calculation gives the expression

$$\sigma_{\alpha\beta} = \pi\lambda_\alpha^2 \left(T_\alpha T_\beta / \sum_i T_i \right). \tag{11.2}$$

This may indeed be proved quite easily from the reciprocity theorem for nuclear reactions and the hypothesis of complete independence of the processes of formation and decay of the compound nucleus. The relation (11.2) is essentially the Hauser–Feshbach formula, though much more detailed expressions must be used in practical calculations.

This shows that the compound nucleus cross section can be calculated provided the transmission coefficients in all the open reaction channels are known. These can be calculated from the appropriate optical potentials, and in the case of channels other than the entrance and exit channels of the reaction being considered it is usually sufficiently accurate to use overall optical potentials. For the entrance and exit channels it is desirable to use potentials fitted to the relevant data. In many compound nucleus reactions the number of open channels is exceedingly large, so that it is not practicable to calculate the transmission coefficient for each of them individually. It is then sufficiently accurate to separate the denominator of (11.2) into two parts

$$\sum_i T_i = \sum_i{}' T_i + \sum_j \int \omega(E)\, T_j(E)\, \mathrm{d}E \tag{11.3}$$

where the first term refers to the important channels that can be treated individually and the second term is an integral over the regions where there are a large number of levels with level density $\omega(E)$ and transmission coefficient $T_j(E)$.

Several refinements to the Hauser–Feshbach calculation have been developed in recent years. The most important is the width fluctuation correction, which takes

account of the partial breakdown of the hypothesis of the independence of the processes of formation and decay of the compound nucleus. This is done by multiplying the contribution to the cross section from each channel by the factor

$$W_{\alpha\beta} = \left\langle \frac{\Gamma_\alpha \Gamma_\beta}{\Gamma} \right\rangle \Big/ \frac{\langle \Gamma_\alpha \rangle \langle \Gamma_\beta \rangle}{\langle \Gamma \rangle} \tag{11.4}$$

where the Γ_i are widths and $\Gamma = \sum_i \Gamma_i$. For $\langle \Gamma_\alpha \rangle \ll D$, where D is the mean separation of the compound nucleus levels and the angular brackets indicate energy-averaging. The widths are related to the transmission coefficients by

$$T_\alpha \simeq \frac{2\pi \langle \Gamma_\alpha \rangle}{D}. \tag{11.5}$$

This width fluctuation correction factor may be calculated from the probability distribution of the nuclear levels. By using the Porter–Thomas distribution

$$P(x)\,\mathrm{d}x = (2\pi x)^{-1/2}\,\mathrm{e}^{-x/2}\,\mathrm{d}x \tag{11.6}$$

where $x = \Gamma/\langle \Gamma \rangle$, an explicit expression may be obtained for the width fluctuation correction, and this may be evaluated numerically from the values of the transmission coefficients. Several comparisons between compound nucleus calculations and experimental data show the necessity of including the width fluctuation correction (Hellström *et al* 1970).

There are some other corrections, notably the resonance interference correction (Moldauer 1964a,b), that are sometimes included in Hauser–Feshbach calculations, but they may not be significant in view of an unavoidable difficulty that arises in most cases from the presence of direct nonelastic reactions, which take flux directly from the elastic channels. This makes it incorrect to assume that all the nonelastic flux enters the compound nucleus, and if this is done the resulting compound nucleus cross sections will be too high. It is possible in principle to allow for this by computing the direct nonelastic flux and subtracting it from the total nonelastic flux to get the true flux entering the compound nucleus. Unfortunately this is nearly always impracticable since it requires a detailed theory of all the direct processes and also knowledge of all the corresponding spectroscopic factors, and this is seldom available. This effect may be allowed for in an approximate way by defining a reduction factor R

$$\sigma = \sigma_{\mathrm{DI}} + R\sigma_{\mathrm{CN}} \tag{11.7}$$

where σ_{DI} is the total direct nonelastic cross section and σ_{CN} the total compound nucleus cross section. If R is assumed to be the same in all channels, it may be determined from a comparison of theory and experiment in those reaction channels with no direct contribution and then used to analyse the data in the other channels, including the elastic channels. It is, however, unlikely that the reduction factor is the same in all channels, since the direct processes may be expected to take proportionately more flux from the higher partial waves. Nevertheless the approximation remains a useful one.

The analysis of an elastic scattering cross section with a substantial compound nucleus component must be made iteratively since the optical potential must be known in order to calculate the compound nucleus cross section. In practice, a suitable overall potential is first used to calculate the compound elastic cross sections, and with an assumed value of the reduction factor the shape elastic cross section is

obtained. This is used as the input data for an optical model analysis in which the reduction factor as well as the usual optical model parameters are varied systematically to optimize the fit. With the resulting potential a new compound nucleus cross section is calculated and the whole process repeated until consistency is attained. The result of an analysis of the differential cross section for the elastic scattering of 5 MeV protons by ^{25}Mg, obtained in this way, is shown in figure 28.

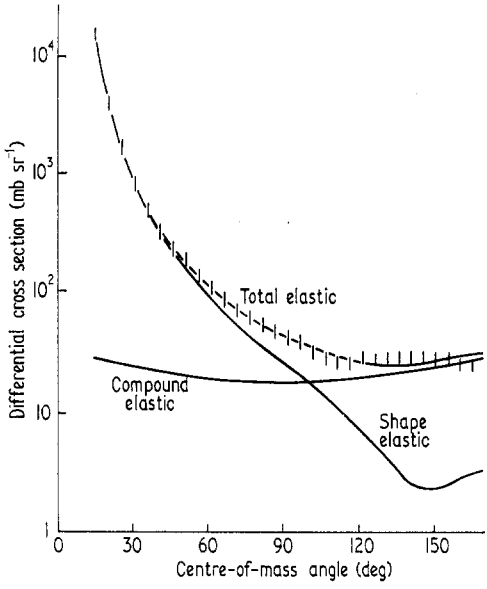

Figure 28. Differential cross section for the elastic scattering of 6 MeV protons by ^{25}Mg analysed into its shape elastic and compound elastic components. The compound elastic cross section was calculated using the Hauser-Feshbach theory including the width fluctuation correction. From Gallmann *et al* (1966).

12. Direct reactions

Many methods of calculating the cross sections of direct reactions have been developed over the last few decades and, as some of the more successful make use of wavefunctions calculated from optical potentials, it is appropriate to mention them here.

Typically, the cross section of a direct nuclear reaction is proportional to the square of a matrix element that may be written schematically in the form

$$M = \langle f | H | i \rangle \tag{12.1}$$

where $|i\rangle$ and $\langle f|$ are the wavefunctions of the initial and final systems and H the part of the hamiltonian responsible for the transition. Thus, for example, in the case of inelastic scattering, $|i\rangle$ is the product of the wavefunctions of the incident particle and the target nucleus in its ground state, and similarly for $|f\rangle$. In the case of a nucleon transfer reaction, such as a (d, p) stripping reaction, $|i\rangle$ is the product of the wavefunction of the incident deuteron, including its internal wavefunction, and that of the target nucleus and $|f\rangle$ represents the wavefunctions of the outgoing proton, the captured neutron and the residual nucleus. In all the expressions, the wavefunction representing the motion of the ingoing and outgoing particles can be

calculated from the Schrödinger equation with the appropriate optical potential, and thus the optical model is an essential part of such theories.

There are several questions that arise concerning this use of optical model wavefunctions. One of the most important is how to justify the use of wavefunctions in the nuclear interior, when the potential from which they are calculated is obtained from elastic scattering that depends only on their asymptotic form in the region beyond the nucleus. There seems to be no way of knowing what the wavefunctions are in the nuclear interior, and yet it is just in this region that they contribute significantly to the direct reaction matrix element. Indeed in the case of deuterons and other composite particles it is difficult to see what meaning can be attached to the wavefunction in the nuclear interior. There is no easy answer to this question, but at least it can be said that the use of such wavefunctions often gives surprisingly good results in direct reaction calculations.

In other cases the distorted wave theory fails, and such situations can be dealt with in several ways. Thus, for example, it is sometimes possible to obtain agreement with experiment by an arbitrary modification of the distorted wave theory, such as imposing a radial cutoff on the overlap integral and ignoring contributions from smaller radii. This device is often successful, but it is unsatisfactory because it is arbitrary, and also because in some cases the cutoff radius is so large as to make the calculations unphysical. Thus the ^{208}Pb(p, d) cross-sections at 22 MeV can be fitted by the distorted wave theory only with a cutoff of 8·5 fm, which is well beyond the nuclear surface.

Another method of tackling failures of the distorted wave theory is to refine the theory itself, and there have been many attempts to do this, by taking into account processes that are normally ignored, such as the possibility of deuteron breakup in the case of (d, p) stripping. The formalism of such refined theory often gives a new prescription for the optical potentials describing the motion of the interacting particles. Using these potentials the old formalism can still be used but effects previously ignored are now included at least approximately.

A calculation of this type has been made for (d, p) stripping by Johnson and Soper (1970). They take into account the deuterons which have been broken up in the average field of the target but whose constituent nucleons continue to move together in a ^{3}S state with little relative momentum, and obtain an expression for the deuteron optical potential $U_d(\boldsymbol{r})$ in terms of the neutron and proton optical potentials $U_n(\boldsymbol{r})$ and $U_p(\boldsymbol{r})$ at half the deuteron energy

$$U_d(\boldsymbol{r}) = D_0^{-1} \int \{U_n(\boldsymbol{r}+\tfrac{1}{2}\boldsymbol{s}) + U_p(\boldsymbol{r}-\tfrac{1}{2}\boldsymbol{s})\} V_{np}(s)\, \phi_d(\boldsymbol{s})\, d\boldsymbol{s} \qquad (12.2)$$

where

$$D_0 = \int V_{np}(\boldsymbol{s})\, \phi_d(\boldsymbol{s})\, d\boldsymbol{s} \qquad (12.3)$$

$V_{np}(\boldsymbol{s})$ is the neutron–proton interaction, $\phi_d(\boldsymbol{s})$ the internal wavefunction of the deuteron in its ground state and $\boldsymbol{s}$ is the relative separation of the neutron and proton in the deuteron. In the limit of the zero-range neutron–proton interaction, this is just the sum of the neutron and proton potentials.

This deuteron potential differs from those found phenomenologically—in particular it has a larger surface diffuseness—and when used in the distorted wave theory it gives excellent results even for cases where the usual theory with optical

potentials fitted to the elastic scattering fails. For the ^{208}Pb(p, d) reaction mentioned above, for example, it gives a good fit without a radial cutoff, and acceptable spectroscopic factors (Satchler, 1971b). Such an improvement has also been found for similar reactions on light nuclei (Johnson and Soper 1970). Further investigations are required, but already it seems likely that this prescription for the deuteron optical potential is a significant improvement on the usual distorted wave theory, and thus should be a useful tool in nuclear structure studies.

A second question concerns the effect of the nonlocality of the potential. As mentioned in § 1, the optical potential is partially nonlocal, though for convenience it is usual to work with the equivalent local potentials. While the wavefunctions corresponding to these potentials are by definition the same in the asymptotic region, they differ significantly in the nuclear interior. Indeed Perey (1962) has shown that to a good approximation

$$\psi_{\mathrm{NL}}(r) = \frac{\psi_{\mathrm{L}}(r)}{\{1+(2m\beta^2/\hbar^2)\,V(r)\}^{1/2}} \tag{12.4}$$

where $V(r)$ is the equivalent local potential and β the range of the nonlocality. The effect of this is to reduce $\psi_{\mathrm{L}}(r)$ by a factor that can be as much as 20% in the centre of the nucleus, falling to zero in the surface region. Using this expression the wavefunction can be corrected for the nonlocality, and calculations made with this correction show improved accord with the experimental data.

A final question regards the optical potential that should be used to describe the interaction of a particle with an excited nucleus, for this is needed whenever the residual nucleus is not in its ground state. This cannot be investigated experimentally, and at present there seems to be no strong theoretical reason for supposing that the optical potential depends at all strongly on the state of nuclear excitation, so it is usual to assume the dependence to be negligible. The error in so doing is certainly less than the other uncertainties in direct reaction calculations.

An attempt to calculate the potential due to an excited nucleus and to evaluate the effect of any difference from the ground-state potential has recently been made by Cooper *et al* (1971). They studied the ^{16}O(d, p)^{17}O* reaction and calculated the ^{17}O potential by adding the potential due to the valence neutron to the phenomenological optical potential. The potentials corresponding to the neutrons in the $1d_{5/2}$ and $2s_{1/2}$ state were calculated for this purpose using the Reid soft core potential and a Faddeev impulse approximation. The resulting ^{17}O potential gave a stripping cross section to the ground state similar to that obtained with a phenomenological ^{17}O optical potential, and reduced the cross section of the reaction to the excited state by a few per cent.

13. The future development of the optical model

The optical model has enjoyed impressive success over the last two decades, and it is worthwhile trying to outline the main lines of future development. It is convenient to begin with the model as applied to nucleon elastic scattering, and then to consider more complicated circumstances.

The optical model is able to give precision fits to elastic scattering differential cross sections, polarizations, reaction cross sections and (for neutrons) total cross sections, provided the phenomenological parameters are optimized for each nucleus at each energy. These particular potentials may be useful for some purposes, but it

is obviously desirable to have an overall potential that fits the scattering from many nuclei at many energies with the same parameters. Such potentials have been found, subject to certain restrictions, but the corresponding fits are not quite as good, though still very satisfactory and useful for many applications. These overall phenomenological potentials have been progressively refined with the addition of isospin and other small terms, and include allowance for the energy dependence of the parameters.

These phenomenological potentials, both particular and overall, have several disadvantages. In general they are overparametrized, especially at low energies, so that many different potentials can be found to give equally good fits to the data. This poses the question of the physical content of the potentials, and raises doubts about the reliability of the distorted waves that are frequently calculated from them and used in reaction calculations.

It is of course to be expected that the particular potentials give better fits than the overall ones because they can take account of effects connected with the particular structure of the nucleus concerned, though at the expense of the generality of the model. The question to be faced is whether to use particular potentials for the sake of accuracy and accept the loss of generality and the large number of parameters, or whether to use overall potentials and try to refine them with the addition of more small terms, in both cases accepting the uncertainties connected with the ambiguities.

The way out of this impasse is to strengthen the physical basis of the potential by calculating it from the known nuclear characteristics and the nucleon–nucleon interaction. Ideally this could eliminate the ambiguities and also give the required sensitivity to details of nuclear structure without many arbitrary parameters. There are formidable difficulties in carrying out this programme, but the successes that have already been attained show that it is worth pursuing.

In its simplest form this approach gives the real part of the optical potential as an overlap integral of the nuclear density distribution and the nucleon–nucleon interaction. Together with a phenomenological imaginary potential this is able to give a fair account of the data for medium and heavy nuclei at energies of tens of MeV where some of the effects that are neglected, especially antisymmetrization and core polarization, are small. Further progress is being made by calculating these effects, and adding them to the first-order terms already known. Such calculations naturally require more or less detailed nuclear structure information, and thus provide a link between optical model calculations and the work on the nuclear charge and density distributions and on the nucleon–nucleon interaction. The aim of this work is to provide a perfectly general way of calculating the optical potential for any nucleus, including the spin–orbit, isospin and spin–spin terms and the energy dependence. It is not expressed in the usual Saxon–Woods form, as each term will have its own radial dependence, which will vary from one nucleus to the next depending on the differences in nuclear structure. Thus the simplicity of the old optical model is lost, but with a corresponding gain in physical reliability.

These remarks apply to the real part of the optical potential. The imaginary part poses a more complicated problem, and although many detailed attempts have been made to calculate it, a satisfactory way of doing so is still far away. This is only to be expected, since this part of the potential takes account of all the non-elastic processes, and these usually include many different types of reactions. Fortunately from one point of view, the elastic scattering is insensitive to the form

chosen for the imaginary part of the potential, provided the parameters are optimized. This part of the potential will continue to be treated phenomenologically for the foreseeable future, and it may be possible to establish reliable expressions giving the variation of the parameters of this potential as a function of energy and from nucleus to nucleus.

A similar programme of work can be envisaged for the optical potentials for composite particles, with the additional complications due to their internal structure. Such potentials can in principle be calculated either directly from the nucleon–nucleon interaction and the structures of the nucleus and the incident particles or by making use of the nucleon–nucleus potentials as an intermediate step. The latter approach has been used most frequently so far, and significant progress has been made.

A further account of many of the questions discussed here, together with more extensive references, may be found in the review by Hodgson (1971).

Acknowledgment

I gratefully acknowledge the permission of the Clarendon Press to reproduce some figures from my book *Nuclear Reactions and Nuclear Structure.*

References

AFNAN I R and TANG Y C 1970 *Nucl. Phys.* A **141** 653
BANG J and ZIMANYI J 1969 *Nucl. Phys.* A **139** 534
BARSCHALL H H 1952 *Phys. Rev.* **86** 431
BATTY C J and GREENLEES G W 1969 *Nucl. Phys.* A **133** 673
BATTY C J and TSCHALÄR C 1970 *Nucl. Phys.* A **143** 151
BECCHETTI F D and GREENLEES G W 1969 *Annual Report of the J H Williams Laboratory of Nuclear Physics, University of Minnesota* 116
BENCZE GY and DOLESCHALL P 1970 *Phys. Lett.* **32B** 539
BETHE H A 1956 *Phys. Rev.* **103** 1353
BISSON A E, EBERHARD K A and DAVIS R H 1970 *Phys. Rev.* C **1** 539
BOYD R N *et al* 1971 *Nucl. Phys.* A **162** 497
BROWN G E, GUNN J H and GOULD P 1963 *Nucl. Phys.* **46** 598
BRUECKNER K A 1954 *Phys. Rev.* **96** 508
see also BRUECKNER K A, EDEN R J and FRANCIS N C 1955 *Phys. Rev.* **99** 76
—— 1955 *Phys. Rev.* **100** 891
BRUECKNER K A and LEVINSON C A 1955 *Phys. Rev.* **97** 1344
BRUECKNER K A, LOCKETT A M and ROTENBERG M 1961 *Phys. Rev.* **121** 255
BUCK B 1963 *Phys. Rev.* **130** 712
BUCK B, STAMP A P and HODGSON P E 1963 *Phil. Mag.* **8** 1805
BUDZANOWSKI A *et al* 1967 *Proc.* 1966 *Gatlinburg Int. Nucl. Phys. Conf.* ed R L Becker *et al* (New York: Academic Press) p81
BUDZANOWSKI A *et al* 1969 *Nucl. Phys.* A **126** 369
BUDZANOWSKI A, DUDEK A, GROTOWSKI K and STRZALKOWSKI A 1970 *Phys. Lett.* **32B** 431
CHATWIN R A, ECK J S, ROBSON D and RICHTER A 1970 *Phys. Rev.* C **1** 795
COHEN B L 1965 *Am. J. Phys.* **33** 1011
COLE B J, HUBY R and MINES J R 1970 *Phys. Lett.* **33B** 320
COOPER M D, LERNER G M and REDISH E C 1971 *Bull. Am. Phys. Soc.* **16** 99
DUDEK A and HODGSON P E 1972 *J. Phys., Paris* (in press)
EBERHARD K A 1970 *Phys. Lett.* **33B** 343
EBERHARD K A and ROBSON D 1971 *Phys. Rev.* C **3** 149
ELTON L R B 1968 *Phys. Lett.* **26B** 689
FARAGGI H *et al* 1971 *Ann. Phys.* **66** 905
FERNANDEZ B and BLAIR J S 1970 *Phys. Rev.* C **1** 523

FERNBACH S, SERBER R and TAYLOR T B 1949 *Phys. Rev.* **75** 1352
FESHBACH H 1958a *A. Rev. Nucl. Sci.* **8** 49
—— 1958b *Ann. Phys.* **5** 357
—— 1962 *Ann. Phys.* **19** 287
FESHBACH H, PORTER C E and WEISSKOPF V F 1954 *Phys. Rev.* **96** 448
FISHER T R 1971 *Phys. Lett.* **35B** 573
FISHER T R *et al* 1966 *Phys. Rev. Lett* **17** 36
FORTUNE H T, GRAY T J, TROST W and FLETCHER N R 1969 *Phys. Rev.* **179** 1033
FORTUNE H T and VINCENT C M 1969 *Phys. Rev.* **185** 1401
GALLMANN A *et al* 1966 *Nucl. Phys.* **88** 654
GIBSON E F *et al* 1967 *Phys. Rev.* **155** 1194
GLASGOW D W and FOSTER D G 1971 *Phys. Rev.* C **3** 604
GOLDBERGER M L 1948 *Phys. Rev.* **74** 1269
GREENLEES G W *et al* 1970a *Phys. Rev.* C **2** 1063
GREENLEES G W, MAKOFSKE W and PYLE G J 1970b *Phys. Rev.* C **1** 1145
GREENLEES G W and PYLE G J 1966 *Phys. Rev.* **149** 836
GREENLEES G W, PYLE G J and TANG Y C 1968 *Phys. Lett.* **26B** 658
—— 1969 *Phys. Rev.* **171** 1115
GREENLEES G W and TANG Y C 1971 *Phys. Lett.* **34B** 359
GRIMM R C, MCCARTHY I E and STORER R G 1971 *Nucl. Phys.* A **166** 330
HAUSER W and FESHBACH H 1952 *Phys. Rev.* **87** 366
HÄUSSER O, VON BRENTANO P and MAYER-KUCKUK T 1964 *Phys. Lett.* **12** 226
HELLSTRÖM J, DALLIMORE P J and DAVIDSON W F 1969 *Nucl. Phys.* A **132** 581
HODGSON P E 1961 *Phys. Rev. Lett* **6** 358
—— 1963 *The Optical Model of Elastic Scattering* (Oxford: Clarendon Press)
—— 1966 *Adv. Phys.* **15** 329
—— 1967 *Nucl. Phys.* A **103** 127
—— 1968 *Adv. Phys.* **17** 563
—— 1970 *Nucl. Phys.* A **150** 1
—— 1971 *Nuclear Reactions and Nuclear Structure* (Oxford: Clarendon Press)
HUBY R 1970 *Phys. Lett.* **33B** 323
HUBY R and MINES J R 1965 *Rev. Mod. Phys.* **37** 406
JACKSON D F and KEMBHAVI V K 1969 *Phys. Rev.* **178** 1626
JOHANSSON A, SVANBERG U and HODGSON P E 1961 *Ark. Fys.* **19** 541
JOHNSON R C and SOPER P J R 1970 *Phys. Rev.* C **1** 976
JONES G A 1970 *Rep. Prog. Phys.* **33** 645
KEATON P W 1971 *Los Alamos Report* LA-DC-12739
KIDWAI H R and ROOK J R 1971 *Nucl. Phys.* A **169** 417
KOSSANYI-DEMAY P and MAYER B 1967 *J. Phys.* C: *Solid St. Phys.* **1** 137
LANE A M 1957 *Rev. Mod. Phys.* **29** 191
—— 1962 *Nucl. Phys.* **35** 676
LE LEVIER R E and SAXON D S 1952 *Phys. Rev.* **87** 40
LILLEY J S 1971 *Phys. Rev.* C **3** 2229
MCEVER W S *et al* 1970 *Phys. Rev. Lett.* **24** 1123
MACKINTOSH R D 1971 *Nucl. Phys.* A **164** 398
MELDNER H 1969 *Phys. Rev.* **178** 1815
MIKOSHIBA O, TERASAWA T and TANIFUJI M 1971 *Nucl. Phys.* A **168** 417
MILLENER D J and HODGSON P E 1971 *Phys. Lett.* **35B** 495
MOLDAUER P A 1961 *Phys. Rev.* **123** 968
see also MOLDAUER P A 1967 *Phys. Rev.* **157** 907
—— 1968 *Phys. Rev.* **171** 1164
—— 1969 *Phys. Rev.* **177** 1841
—— 1964a *Rev. Mod. Phys.* **36** 1079
—— 1964b *Phys. Rev.* B **135** 642
MONAHAN J E and ELWYN A J 1964 *Phys. Rev.* B **136** 1678
MORGAN C G and JACKSON W F 1969 *Phys. Rev.* **188** 1758
MUKHERJEE S 1968 *Nucl. Phys.* A **118** 423
NAGAMINE K, UCHIDA A and KOBAYASHI S 1970 *Nucl. Phys.* A **145** 203
NEWSTEAD C M, DELAROCHE J and CANVIN B 1971 *Proc. Albany Conf.* (in press)

OWEN L W and SATCHLER G R 1970 *Phys. Rev. Lett.* **25** 1721
PASCOLINI A, PISENT G and ZARDI F 1969 *Nuovo Cim. Lett.* **1** 643
PEREY C M and PEREY F G 1963 *Phys. Rev.* **132** 755
—— 1968 *Phys. Lett.* **26B** 123
PEREY C M, PEREY F G, DICKENS J K and SILVA R J 1968 *Phys. Rev.* **175** 1460
PEREY F G 1962 *Direct Interactions and Nuclear Reaction Mechanisms* ed E Clementel and C Villi (New York: Gordon and Breach) p125
—— 1963 *Phys. Rev.* **131** 745
—— 1964 *Argonne National Laboratory Report* ANL-6848 114
PEREY F G and BUCK B 1962 *Nucl. Phys.* **32** 353
PYLE G J and GREENLEES G W 1969 *Phys. Rev.* **181** 1444
RAHMAN KAHN M Z 1966 *Nucl. Phys.* **76** 475
RAYNAL J 1963 *Phys. Lett.* **7** 281
REBEL H 1971 *Karlsruhe Cyclotron Laboratory Report* KFK-1397
RIHAN T H and SHARAF M A 1969 *Nucl. Phys.* A **134** 369
ROST E 1968 *Phys. Lett.* **26B** 184
SAMADDAR S K and MUKHERJEE S 1971 *Nucl. Phys.* A (in press)
SAMADDAR S K, SATPATHY R K and MUKHERJEE S 1970 *Nucl. Phys.* A **150** 655
SATCHLER G R 1960 *Nucl. Phys.* **21** 116
—— 1967 *Nucl. Phys.* A **92** 273
—— 1971a *Phys. Lett.* **34B** 37
—— 1971b *Phys. Rev.* C **4** 1485
SATCHLER G R and HAYBRON R M 1964 *Phys. Lett.* **11** 313
SATCHLER G R *et al* 1968 *Nucl. Phys.* A **112** 1
SATPATHY R K, SAMADDAR S K and MUKHERJEE S 1969 *Nucl. Phys.* A **132** 276
SCHIFFER J P 1963 *Nucl. Phys.* **46** 246
SCHMEING N C 1970 *Nucl. Phys.* A **142** 449
SCHWANDT P and HAEBERLI W 1969 *Nucl. Phys.* A **123** 401
SINHA B C and EDWARDS V R W 1970 *Phys. Lett.* **31B** 273
SPRINGER A and HARVEY B G 1965 *Phys. Lett* **14** 116
TAMURA T 1965 *Rev. Mod. Phys.* **37** 679
TANG Y C 1969 *Proc. Bochun Int. Conf. Clustering Phenomena in Nuclei* (Vienna: International Atomic Energy Agency) p109
TESTONI J and GOMES L C 1966 *Nucl. Phys.* **89** 288
THOMPSON W J 1971 *Particles and Nuclei* **2** 47
URONE P P, PUT L W, CHANG H H and RIDLEY B W 1971 *Nucl. Phys.* A **163** 225
WATANABE S 1958 *Nucl. Phys.* **8** 484
WEISSER D C, LILLEY J S, HOBBIE R K and GREENLEES G W 1970 *Phys. Rev.* C **2** 544
WILKINSON D H 1961 *Proc. Rutherford Jubilee Int. Conf.* ed J B Birks (Manchester: Heywood) p339
WILMORE D and HODGSON P E 1964 *Nucl. Phys.* **55** 673
WOOLAM P B, GRIFFITHS R J, GRACE J F and LEWIS V E 1970, *Nucl. Phys.* A **154** 513
YOUNGBLOOD D H, KOZUB R L, KENEFICK R A and HIEBERT J C 1970 *Phys. Rev.* C **2** 477